

 Open access • Journal Article • DOI:10.14359/9680




## Splice strength of high relative rib area reinforcing bars — Source link

David Darwin, Michael L. Tholen, Emmanuel K. Idun, Jun Zuo

**Published on:** 01 Jan 1996 - Aci Structural Journal (University of Kansas Center for Research, Inc.)

Related papers:

- [Splice Strength of Conventional and High Relative Rib Area Bars in Normal and High-Strength Concrete](#)
- [Reevaluation of test data on development length and splices](#)
- [Bond of epoxy-coated reinforcement: bar parameters](#)
- [Effect of Deformation Height and Spacing on Bond Strength of Reinforcing Bars](#)
- [Bond Performance of Reinforcing Bars Embedded in High-Strength Concrete](#)

Share this paper:    

View more about this paper here: <https://typeset.io/papers/splice-strength-of-high-relative-rib-area-reinforcing-bars-40e9j7cnx0>

**SPLICE STRENGTH OF HIGH RELATIVE RIB  
AREA REINFORCING BARS**

**By**  
**David Darwin**  
**Michael L. Tholen**  
**Emmanuel K. Idun**  
**Jun Zuo**

**A Report on Research Sponsored by**  
**THE CIVIL ENGINEERING RESEARCH FOUNDATION**  
**Contract No. 91-N6002**

**THE NATIONAL SCIENCE FOUNDATION**  
**Research Grants No. MSS-9021066 and CMS-9402563**

**THE REINFORCED CONCRETE RESEARCH COUNCIL**  
**Project 56**

**STRUCTURAL ENGINEERING AND ENGINEERING MATERIALS**  
**SL REPORT 95-3**

**UNIVERSITY OF KANSAS CENTER FOR RESEARCH, INC.**  
**LAWRENCE, KANSAS**  
**MAY 1995**

## LEGAL NOTICE

This report was prepared by the University of Kansas Center for Research, Inc. as an account of work sponsored by the Civil Engineering Research Foundation (CERF) and the National Science Foundation (NSF).

Neither CERF, nor any persons acting on behalf of either:

- a. Makes any warranty or representation, express or implied, with respect to the accuracy, completeness, or usefulness of the information contained in this report, or that the use of any apparatus, method, or process disclosed in this report may not infringe third party rights; or
- b. Assumes any liability with respect to the use of, or for damages resulting from the use of, any information, apparatus, method, or process disclosed in this report.
- c. Makes any endorsement, recommendation or preference of specific commercial products, commodities or services which may be referenced in this report.

Any opinions, findings, and conclusions or recommendations expressed in this material are those of the authors and do not necessarily reflect the views of the National Science Foundation.

# SPLICE STRENGTH OF HIGH RELATIVE RIB AREA REINFORCING BARS

## ABSTRACT

The reinforcing bar deformation patterns currently used in the United States were established over forty-five years ago. In the interim, material properties and design procedures have changed, resulting in more congested reinforcement, the use of higher strength materials, and the application of coatings to provide corrosion protection. Based on an improved understanding of the interaction between reinforcing steel and concrete, changes have been made in the design provisions for reinforced concrete buildings and bridges to account more accurately for structural behavior and material properties. However, corresponding changes have not been made in the steel reinforcement.

This report describes the testing and analysis of 83 beam-splice specimens containing No. 5, No. 8, and No. 11 (16, 25, and 36 mm) bars with relative rib areas (ratio of projected rib area normal to bar axis to the product of the nominal bar perimeter and the center-to-center rib spacing) ranging from 0.065 to 0.140. Concretes containing two different coarse aggregates were used to evaluate the effect of aggregate properties on bond strength. Sixty specimens contained uncoated bars with confining transverse reinforcement. Thirteen specimens contained uncoated bars without confining reinforcement, and ten specimens contained epoxy-coated bars, nine without confining reinforcement and one with confining reinforcement. The tests are analyzed to determine the effect of relative rib area and bar diameter on the increase in bond strength provided by confining reinforcement. The tests also provide a preliminary indication of the effect of high relative rib area on the splice strength of epoxy-coated bars.

The splice strength of uncoated reinforcement confined by transverse reinforcement increases with an increase in the relative rib area and the bar diameter of the spliced bars. The increase in splice strength provided by transverse reinforcement increases as the strength of the coarse aggregate increases. The use of reinforcing bars with an average relative rib area of 0.1275, an increase from the value for conventional bars of 0.0727, can provide up to a 26 percent decrease

in splice length compared to conventional reinforcement when confining reinforcement is used. The savings obtainable with high relative rib area bars is highest for low covers and bar spacings. Epoxy coating appears to have a less detrimental effect on splice strength for high relative rib area bars than for conventional bars. The results indicate that the maximum development length modification factor used for epoxy-coated reinforcement may be reduced by 20 percent.

**Keywords:** bond (concrete to reinforcement); bridge specifications; building codes; deformed reinforcement; development; lap connections; reinforcing steels; relative rib area; splicing; structural engineering.

## ACKNOWLEDGEMENTS

Support for this research was provided by the Civil Engineering Research Foundation under CERF Contract No. 91-N6002, the National Science Foundation under NSF Grants No. MSS-9021066 and CMS-9402563, the Reinforced Concrete Research Council under RCRC Project 56, ABC Coating, Inc., Birmingham Steel Corporation, Chaparral Steel Company, Fletcher Coating Company, Florida Steel Corporation, Morton Powder Coatings, Inc., North Star Steel Company, O'Brien Powder Products, Inc., and 3M Corporation. Epoxy coating was applied to the C bars by ABC Coating, Inc., to the F bars by Florida Steel Corporation, and to the N bars by Simcote, Inc. The basalt coarse aggregate was supplied by Iron Mountain Trap Rock Company and Geiger Ready-Mix. Form release agent, curing compound, and mounting hardware were supplied by Richmond Screw Anchor Company.



## INTRODUCTION

The reinforcing bar deformation patterns currently used in the United States were established over forty-five years ago. In the interim, material properties and design procedures have changed, resulting in more congested reinforcement, the use of higher strength materials, and the application of coatings to provide corrosion protection. Based on an improved understanding of the interaction between reinforcing steel and concrete, changes have been made in the design provisions for reinforced concrete buildings and bridges to account more accurately for structural behavior and material properties. However, corresponding changes have not been made in the steel reinforcement.

With the goal of improving the development characteristics of reinforcing steel, studies have been under way since 1991 to accurately characterize the development and splice behavior of current reinforcing bars and to modify the deformation characteristics of the bars to attain improved bond strength (Darwin, McCabe, Idun and Schoenekase 1992a, 1992b, Darwin and Graham 1993a, 1993b). As part of the study, Darwin and Graham (1993a, 1993b) demonstrated that, for uncoated reinforcement, the higher the relative rib area,  $R_r$  (ratio of projected rib area normal to bar axis to the product of the nominal bar perimeter and the center-to-center rib spacing), the higher the bond strength between reinforcing steel and concrete for bars confined by transverse reinforcement. Bars in U.S. practice typically have values of  $R_r$  between 0.06 and 0.08. Using specially machined 1 in. (25 mm) diameter bars with values of  $R_r$  between 0.05 and 0.20, Darwin and Graham observed that the increase in bond strength does not depend on the specific combination of rib height and spacing, but only on the value of  $R_r$ . Deformation pattern was found to have no effect on the bond strength of unconfined bars, matching the findings for uncoated conventional bars in a study by Choi, Hadje-Ghaffari, Darwin and McCabe (1990, 1991). In that earlier study, however, Choi et al. (1990, 1991) did observe that an increase in  $R_r$  resulted in an increase in the bond strength of epoxy-coated bars relative to uncoated bars, even without confining steel. The latter observation suggests that the development lengths of epoxy-coated high  $R_r$  bars might not



have to be increased by 50 percent compared to uncoated bars, as required by the 1989 ACI Building Code and the 1992 AASHTO Bridge Specifications.

The next step in the current study, reported here, involves tests of commercially produced reinforcing bars with high relative rib areas. As with the vast majority of the tests used to establish development length criteria (Chinn et al. 1955, Chamberlin 1956, 1958, Mathey and Watstein 1961, Ferguson and Breen 1965, Ferguson and Thompson 1965, Thompson et al. 1975, Zekany et al. 1981, Choi et al. 1990, 1991, DeVries et al. 1991, Hester et al. 1991, 1993, Rezansoff et al. 1991, 1993, Azizinamini et al. 1993, 1995), the bond strength of these bars was evaluated using splice specimens. The test results, including comparisons with conventional reinforcing bars, are presented in this report. An analysis of the results indicates that significant reductions in development and splice length can be obtained by using reinforcing bars with high relative rib areas.

## EXPERIMENTAL PROGRAM

The experimental program described in this report consisted of 83 beam-splice specimens, cast in 18 groups of 4 to 6 specimens each. The key test parameters were the bar size [No. 5, No. 8, or No. 11 (16, 25 or 36 mm)], the relative rib area (0.065 to 0.140), and the degree of confinement provided by transverse reinforcement. Concretes containing two different coarse aggregates were used to evaluate the effect of aggregate properties on bond strength. Sixty specimens contained uncoated bars with confining reinforcement; thirteen specimens contained uncoated bars without confining reinforcement; and ten specimens contained epoxy-coated bars, nine without confining reinforcement and one with confining reinforcement. The bars used in the study are shown in Figs. 1a and 1b.

### Test Specimens

The splice specimens, 13 or 16 ft long (4 or 4.9 m), were tested as inverted simply supported beams to produce, respectively, a 4 or 6 ft (1.2 or 1.8 m) constant moment region, as

shown in Fig. 2. The specimens contained two to four adjacent bottom-cast splices (Fig. 3). No. 3 or No. 4 (9.5 or 13 mm) closed stirrups were spaced equally within the splice regions to determine the effects of stirrups on splice strength, and No. 3 (9.5 mm) stirrups were placed outside the constant moment region to provide shear strength. One specimen contained two splices and two continuous bars. No. 4, No. 5 and No. 6 (13, 16, and 19 mm) bars were used as top reinforcement for specimens with No. 5, No. 8 and No. 11 (16, 25 and 35 mm) test bars, respectively. The beams had nominal widths of 12 or 18 in. (305 or 457 mm) and nominal depths of 15.5 to 17 in. (394 to 432 mm). Total depths were varied to maintain a nominal effective depth,  $d$ , of  $13\frac{3}{4}$  in. (350 mm). Nominal values for bottom cover varied between 1.25 and 3 in. (32 and 76 mm), and side covers on the splices ranged between 1 and 3 in. (25 and 76 mm). Actual member dimensions are given in Table 1.

## Materials

**Reinforcing Steel**—Bars with both conventional and experimental deformation patterns were evaluated in the study. The bars met the requirements of ASTM A 615, with the exception that some of the experimental bars did not have bar markings. Seven conventional bars and five experimental bars were evaluated. The conventional bars consisted of one No. 5 (16 mm) bar, designated 5N0; four No. 8 (25 mm) bars, designated 8C0, 8N0, 8S0 and 8SH0; and two No. 11 (36 mm) bars designated 11B0 and 11N0. The high relative rib area bars consisted of one No. 5 (16 mm) bar, 5C2; three No. 8 (25 mm) bars, 8C1, 8F1, and 8N3; and one No. 11 (36 mm) bar, 11F3. [Note: The first number in the designation is the bar size; the letter(s) identify the manufacturer; a trailing zero identifies a conventional bar; a nonzero trailing number identifies an experimental deformation pattern.] Bar properties are presented in Table 2. The high  $R_f$  bars have closer and generally higher ribs than the corresponding conventional bars (Figs. 1a and 1b). Conventional ASTM Grade 60 (400 MPa) bars were used as stirrups and top reinforcement.

**Concrete**—Air-entrained concrete was supplied by a local ready mix plant. Two types of coarse aggregate (crushed limestone and basalt) with a  $\frac{3}{4}$  in. (19 mm) maximum nominal size

were used, along with Type I portland cement and Kansas River sand. 1 in. (25 mm) square by 3 in. (152 mm) long specimens of the limestone have compressive strengths of about 15,000 psi (103 MPa), while similar specimens of the basalt have compressive strengths of about 50,000 psi (345 MPa). Water-cement ratios, ranging from 0.36 to 0.45, were used to produce concrete strengths ranging from 3810 to 5250 psi (26 to 36 MPa) at the time of test. Testing ages ranged from 5 to 30 days. Mix proportions and concrete properties are summarized in Table 3.

### **Placement Procedure**

The concrete was placed in two lifts. In the initial lift, the end regions were placed first, followed by the splice regions. In the second lift, the splice regions were placed first. Each lift was vibrated on alternate sides of the beams at staggered 1 ft (0.3 m) intervals.

Standard 6 x 12 in. (152 x 305 mm) test cylinders were cast in steel molds and cured in the same manner as the test specimens. Forms were stripped after the concrete had reached a compressive strength of at least 3000 psi (21 MPa), and the specimens were then left to dry until the time of the test.

### **Test Procedure**

The splice specimens were inverted and tested as shown in Fig. 2. The beams were supported by pin and roller supports mounted on concrete pedestals. Steel plates separated the beams from the supports. Loads were applied at the ends of the cantilever regions. Beams were loaded continuously to failure at a rate of about 3 kips (13 kN) per minute at each end. Deflections were measured at each end and at the middle of the beams using linear variable differential transformers (LVDTs). Tests lasted about 15 minutes.

## SPECIMEN BEHAVIOR AND ANALYSIS OF TEST RESULTS

### Results and Observations

Load-deflection curves for the test specimens are shown in Appendix A. Failure loads, moments and bar stresses are given in Table 1. Beams without stirrups failed suddenly and with little warning. Beams with stirrups behaved ductilely after initial cracking, and ultimately exhibited much more cracking due to splice failure than did beams without stirrups. Beams containing epoxy-coated bars had lower strengths than the corresponding beams with uncoated bars. Typical sections following failure are shown in Figs. 4a and 4b.

Splice failure was preceded by extensive longitudinal and transverse cracking in the splice region. Longitudinal cracks formed first on the tension face of the specimen and later on the sides of the specimen at the level of the splices, terminating at the ends of the splice. At each end of the splice, transverse cracks, normal to the longitudinal cracks on the tension surface, ran across the full width of the beam, extending to the sides.

Following the tests, the concrete cover was removed to study the nature of the interaction at the steel-concrete interface. For uncoated bar specimens, both with and without stirrups, the concrete between the ribs at the concrete-steel interface showed signs of crushing. Concrete damage between ribs was higher near the discontinuous end of the spliced bars than near the continuous end. For the high  $R_r$  bars, the concrete failure looked more like a shear failure than a crushing failure, with sections of the concrete remaining intact between the ribs. On a number of specimens, the concrete between the ribs near the "loaded" end of the splice showed little damage – as if the bars had been removed cleanly. Concrete near the discontinuous end of the splice showed progressively more damage. This type of failure was more evident for the new No. 11 bars (36 mm) (designated 11F3) confined by stirrups than for the other cases.

For the epoxy-coated bar specimens, the concrete at the interface had a smooth, glassy surface and exhibited little local damage.

## Evaluation of Test Results – Uncoated Bars

The splice strengths obtained with the new high relative rib area,  $R_r$ , bars are compared to tests of conventional bars performed at the University of Kansas with similar concretes (Choi et al. 1990, 1991, Hester et al. 1991, 1993) and with the results of a statistical analysis of a wide range of tests performed in North America over the past forty years (Chinn et al. 1955, Chamberlin 1956, 1958, Mathey and Watstein 1961, Ferguson and Breen 1965, Ferguson and Thompson 1965, Thompson et al. 1975, Zekany et al. 1981, DeVries et al. 1991, Rezansoff et al. 1991, 1993, Azizinamini et al. 1993, 1995), including those reported here. The details of the statistical analysis are presented by Darwin, Zuo, Tholen and Idun (1995).

The comparisons show that, as predicted by Darwin and Graham (1993a, 1993b), an increase in  $R_r$  has no effect on the splice strength of bars (with typical covers) that are not confined by transverse reinforcement, but has a positive effect on the splice strength of bars that are confined.

In the analyses that follow, the total force in a bar at splice failure,  $T_b$ , is taken as the sum of a concrete contribution,  $T_c$ , and a confining steel contribution,  $T_s$ .

The comparisons use the results of a statistical analysis of the results of 133 development and splice tests of bottom-cast bars without confining transverse reinforcement and 166 tests with confining transverse reinforcement (Darwin et al. 1995). Based on that analysis, the ultimate bond force of bars not confined by transverse reinforcement,  $T_c$  (the concrete contribution), can be expressed as

$$\frac{T_c}{f'_c{}^{1/4}} = \frac{A_b f_s}{f'_c{}^{1/4}} = [63 l_d (c_m + 0.5 d_b) + 2130 A_b] \left( 0.01 \frac{c_M}{c_m} + 0.9 \right) \quad (1)$$

in which  $A_b$  = bar area, in in.<sup>2</sup>

$f_s$  = steel stress at failure, in psi

$f'_c$  = concrete compressive strength, in psi;  $f'_c{}^{1/4}$  in psi

$l_d$  = development or splice length, in in.

$c_m, c_M$  = minimum or maximum value of  $c_s$  or  $c_b$  ( $c_M/c_m \leq 3.5$ ), in in.

$c_s$  =  $\min(c_{si} + 0.25 \text{ in.}, c_{so})$ , in in.

$c_{si}$  = one-half of clear spacing between bars, in in.

$c_{so}, c_b$  = side cover or bottom cover of reinforcing bars, in in.

$d_b$  = bar diameter

As shown in Eq. 1, a key observation of the analysis is that splice and development strength is better represented as a function of the 1/4 power of the concrete compressive strength than by the square root of the strength, as traditionally assumed (ACI 318-89).

*Splices Not Confined by Transverse Reinforcement*—During the course of the study, the results of the splice tests for high  $R_f$  bars not confined by transverse reinforcement were found to differ little from the results of similar tests using conventional bars. As a result, the current tests were included in the data base used to develop Eq. 1.

The lack of sensitivity of splice strength to  $R_f$  for unconfined bars is demonstrated by twelve tests with high  $R_f$  bars (two with 5C2 bars, four with 8C1 bars, three with 8F1 bars, one with 8N3 bars, and two with 11F3 bars) performed in this study. The average test/prediction ratio for the twelve tests, based on Eq. 1, is 1.00, compared to an average ratio of 1.02 for sixteen tests performed at the University of Kansas using conventional reinforcement [one in this study, eight by Choi et al. (1990, 1991) and seven by Hester et al. (1991, 1993)] and an average ratio of 1.00 for all 133 tests used to develop Eq. 1.

*Splices Confined by Transverse Reinforcement*—Transverse reinforcement increases splice strength. To calculate the increase in strength resulting from the presence of transverse steel,  $T_s$ , the concrete contribution,  $T_c$  (represented by Eq. 1), is subtracted from the experimentally determined force in a bar at splice failure,  $T_b$ .

The statistical analysis by Darwin et al. (1995) demonstrates that  $T_s$ , normalized with respect to  $f'_c{}^{1/4}$ , depends principally on the “effective transverse reinforcement,”  $NA_{tr}/n$ , in which  $N$  = the number of transverse reinforcing bars (stirrups or ties) crossing  $l_d$ ;  $A_{tr}$  = area of each stirrup or tie crossing the potential plane of splitting adjacent to the reinforcement being developed

or spliced, in in.<sup>2</sup>; and  $n$  = number of bars being developed or spliced along the plane of splitting. The value of  $n$  is determined by the smaller of  $c_b$  or  $c_s$ . If  $c_b$  controls, the plane of splitting passes through the cover and  $n = 1$ . If  $c_s$  controls, the plane of splitting intersects all of the bars and  $n$  = the total number of bars spliced or developed at one location. The analysis (Darwin et al. 1995) demonstrates that  $T_s$  does not depend on the yield strength of transverse reinforcement,  $f_{yt}$ . This result is supported by experimental observations that show that transverse reinforcement rarely yields due to a bond failure (Maeda et al. 1991, Sakurada et al. 1993, Azizinamini et al. 1995). Therefore, it is the total area, not the total yield force, of the confining steel that governs the increase in bond force provided by transverse steel,  $T_s$ .

Comparisons of  $T_s/f'_c{}^{1/4}$  with  $NA_v/n$  for the splices in the current study are presented in Figs. 5 and 6 for the concretes containing limestone and basalt coarse aggregates, respectively. The tests are treated separately because the concrete containing the high compressive strength basalt provides significantly higher bond strengths than does the concrete containing the lower compressive strength limestone, even though the compressive strengths of the concretes are the same. The slopes,  $m$ , and intercepts,  $b$ , of the best-fit lines are presented in Table 4.

Fig. 5 illustrates that the increase in bond strength provided by transverse steel,  $T_s$ , increases with increasing size of the spliced bar, as well as with increasing relative rib area. The results shown in Fig. 5 include the tests performed in this study, along with 10 tests performed by Hester et al. (1991, 1993) using concrete with the same type of coarse aggregate (test data in Appendix B). The smallest contribution from transverse reinforcement is obtained by the conventional No. 5 (16 mm) bars with  $R_r = 0.082$ , followed by the 5C2 No. 5 (16 mm) bars with  $R_r = 0.109$ , the conventional No. 8 (25 mm) bars with  $R_r = 0.065$  to  $0.085$ , the 8C1 No. 8 (25 mm) bars with  $R_r = 0.101$ , the conventional No. 11 (36 mm) bars with  $R_r = 0.070$  and  $0.072$ , the 8F1 No. 8 (25 mm) bars with  $R_r = 0.140$ , and finally the 11F3 No. 11 (36 mm) bars with  $R_r = 0.127$ .

The relationships shown in Fig. 5 suggest that an increase in the wedging action of the bars, resulting from both an increase in  $R_r$  (a relative measure of rib size and spacing) and an increase in the bar size (an absolute measure of rib size) will increase the stress in the stirrups,

resulting in an increase in the confining force. A relationship between confinement and the degree of wedging action is in concert with the observation that stirrups do not yield (Maeda et al. 1991, Sakurada et al. 1993, Azizinamini et al. 1995), allowing an increase in lateral displacement to be translated into an increase in confining force.

The results for the splices cast in concrete containing basalt are shown in Fig. 6. Only No. 8 (25 mm) bars were evaluated using this concrete. As demonstrated in Fig. 5,  $T_s$  increases with increasing relative rib area. The sensitivity of bond strength to coarse aggregate properties is shown in Fig. 7, where the results for bars cast in both types of concrete [conventional bars ( $R_r = 0.065$  to  $0.085$ ) and 8F1 bars ( $R_r = 0.140$ )] are compared. On the average, transverse reinforcement is 35 percent more effective for the conventional reinforcement and 46 percent more effective for the high relative rib area bars for the concrete containing basalt coarse aggregate than for the concrete containing limestone. This sensitivity of bond strength to concrete properties, as affected by the properties of the coarse aggregate, is not widely recognized.

### Application of Test Results to Design – Uncoated Bars

The test results shown in Figs. 5 and 6 serve as the basis for the development of design criteria for high  $R_r$  bars. To accomplish this, the effects of  $R_r$  and bar size must be separated.

*Effect of Relative Rib Area*—As a first step, it is assumed that changes in  $T_s$  caused by changes in  $R_r$  are independent of bar size and concrete properties. To test this assumption, the results in Figs. 5 and 6 are first modified so that the relationships between  $T_s$  and  $NA_{tr}/n$  are expressed as linear functions with zero intercepts at  $NA_{tr}/n = 0$ . These linear functions take the form

$$\frac{T_s}{f'_c{}^{1/4}} = \frac{(2m + b)}{2} \frac{NA_{tr}}{n} = M \frac{NA_{tr}}{n} \quad (2)$$

in which  $m$  and  $b$  = the slope and intercept, respectively, of the best-fit lines shown in Figs. 5 and 6 (Table 4). The representation provided by Eq. 2 will be conservative for test results with a positive intercept,  $b$ , and thus will be conservative for the development of design criteria based on



the new high  $R_r$  bars. The advantage of an expression of the form shown in Eq. 2 is that the combined effects of  $R_r$  and bar size on  $T_s$  can be represented by a single number,  $M$ , the slope of the modified relationship.

The values of  $M$  developed using Eq. 2 are plotted versus  $R_r$  in Fig. 8 for the No. 5, No. 8, and No. 11 (16, 25, and 36 mm) bars shown in Fig. 5 and the No. 8 bars shown in Fig. 6. For each data point, the value of  $R_r$  represents a single value, with the exception of the conventional No. 8 and No. 11 (25 and 36 mm) bars which use a weighted average, since a range of values was used for these tests.

Best-fit lines relating  $M$  to  $R_r$  are obtained for each of the four sets of data and used to establish the value of  $M$  corresponding to  $R_r = 0.075$ , midway in the range used for conventional bars in this study. [Note: The average value of  $R_r$  obtained in a survey of steel from 28 heats, produced by 6 steel mills, for bar sizes No. 5, No. 6, No. 8, and No. 11, and metric bar sizes No. 20, No. 25, No. 30, and No. 35 is 0.0727 (Darwin et al. 1995).] The individual values of  $M$  are then normalized with respect to  $M$  for  $R_r = 0.075$  to obtain the factor  $t_r = M/M_{R_r = 0.075}$  for each set of data. The normalization process should, presumably, remove the effects of bar size and concrete properties, and  $t_r$  should reflect only the effect of relative rib area on  $T_s$ .

The values of  $t_r$  are plotted versus  $R_r$  in Fig. 9. Each data point is weighted based on the number of tests represented. Based on the best-fit line, the relationship between  $t_r$  and  $R_r$  is

$$t_r = 9.6 R_r + 0.28 \quad (3)$$

with a coefficient of determination  $r^2 = 0.966$  (Note:  $t_r = 1$  for  $R_r = 0.075$ ).

The strongly linear relationship between  $t_r$  and  $R_r$  supports the accuracy of the initial assumption that the effects of  $R_r$  are independent of bar size and concrete properties.

**Effect of Bar Size**—Once the effect of relative rib area has been determined, the next step is to determine the effect of bar size on  $T_s$ . This is done by dividing the values of  $M$  by  $t_r$  from Eq.

3, thus converting the original values of  $M$  to values corresponding to bars with  $R_r = 0.075$ . If the resulting values of  $M/t_r$  for a single concrete are used in a regression analysis versus the bar diameter,  $d_b$ , the equation of the best-fit line will give a relationship that represents the effect of bar diameter on  $T_s$  for that concrete. For the bars cast in limestone concrete (Fig. 10), the resulting expression is

$$\frac{M}{t_r} = 1189 d_b + 457 \quad (4)$$

with  $r^2 = 0.974$ .

To generalize this relationship for other concretes (an assumption at this point), Eq. 4 is normalized with respect to  $M/t_r$  for  $d_b = 1$  in. to obtain a term representing the effect of bar size on  $T_s$ .

$$t_d = 0.72 d_b + 0.28 \quad (5)$$

The final result of the analysis is a combined variable that includes the effects of relative rib area, bar diameter, and transverse steel.

$$t_r t_d \frac{NA_{tr}}{n} = (9.6 R_r + 0.28)(0.72 d_b + 0.28) \frac{NA_{tr}}{n} \quad (6)$$

The individual values of  $M$ ,  $t_r$ , and  $M/t_r$  used to develop Eqs. 3-6 are summarized in Table 4.

**Increase in Splice Strength**—When Eq. 6 was used in the statistical analysis of the results of 166 development and splice tests for bars confined by transverse reinforcement, including the 60 tests from this study (Darwin et al. 1995), the resulting best-fit line was

$$\frac{T_s}{f'_c{}^{1/4}} = 2226 (9.6 R_r + 0.28)(0.72 d_b + 0.28) \frac{NA_{tr}}{n} + 66 \quad (7a)$$

$$\frac{T_s}{f'_c{}^{1/4}} = 2226 t_r t_d \frac{NA_{tr}}{n} + 66 \quad (7b)$$

with  $r^2 = 0.856$ .

When used in conjunction with Eq. 1 to calculate total bond force,  $T_b = T_c + T_s$ , Eq. 7 produced a mean test/prediction ratio 1.01 and a coefficient of variation of 0.125 (Darwin et al. 1995).

For conventional reinforcement (average  $R_r = 0.0727$ ), Eq. 7a (dropping the final term, 66) becomes

$$\frac{T_s}{f'_c{}^{1/4}} = 2175 (0.72 d_b + 0.28) \frac{NA_{tr}}{n} \quad (9)$$

*Recommended Value of  $R_r$* —Experience obtained during this study has demonstrated that bars with relative rib areas as high as 0.14 can be rolled successfully using current technology. However, a minimum value of  $R_r = 0.12$  appears to be a good starting point for the new bars in practice, because the difficulty in rolling increases with increases in  $R_r$  and because steel mills will need to shoot for higher values of  $R_r$  to insure a minimum of 0.12. Assuming that the standard deviation in  $R_r$  for the new reinforcement will be one-half of that for conventional bars (Darwin et al. 1995) means that an average value of  $R_r = 0.1275$  will be needed to insure that not more than 5 percent of all bars will have a value of  $R_r < 0.12$ . For an average relative rib area of 0.1275, Eq. 7a (dropping the final term) becomes

$$\frac{T_s}{f'_c{}^{1/4}} = 3350 (0.72 d_b + 0.28) \frac{NA_{tr}}{n} \quad (10)$$

representing a 54 percent increase in the average contribution of transverse reinforcement to  $T_b$  compared to that obtained with conventional bars (Eq. 9).

*Development Length Criteria*—Combining Eqs. 1 and 7b (dropping the final term in Eq. 7b) provides an expression for  $T_b$ .

$$\frac{T_b}{f_c'^{1/4}} = \frac{T_c + T_s}{f_c'^{1/4}} = \frac{A_b f_s}{f_c'^{1/4}} = [63 l_d (c_m + 0.5 d_b) + 2130 A_b] \left( 0.1 \frac{c_M}{c_m} + 0.9 \right) + 2226 t_r t_d \frac{N A_{tr}}{n} \quad (11)$$

Eq. 11 can be converted to an expression for development length,  $l_d$ , by substituting the yield strength,  $f_y$ , for  $f_s$  and  $l_d/s$  for  $N$ , in which  $s$  = spacing of transverse reinforcement in in., and solving for  $l_d$ .

$$l_d = \frac{A_b \left[ \frac{f_y}{f_c'^{1/4}} - 2130 \left( 0.1 \frac{c_M}{c_m} + 0.9 \right) \right]}{63 \left[ (c_m + 0.5 d_b) \left( 0.1 \frac{c_M}{c_m} + 0.9 \right) + \frac{35.3 t_r t_d A_{tr}}{sn} \right]} \quad (12)$$

Eq. 12 can be altered to express  $l_d$  as a multiple of the bar diameter,  $d_b$ .

$$\frac{l_d}{d_b} = \frac{\frac{f_y}{f_c'^{1/4}} - 2130 \left( 0.1 \frac{c_M}{c_m} + 0.9 \right)}{\frac{80.2}{d_b} \left[ (c_m + 0.5 d_b) \left( 0.1 \frac{c_M}{c_m} + 0.9 \right) + \frac{35.3 t_r t_d A_{tr}}{sn} \right]} \quad (13)$$

Eq. 13 can be simplified further by setting  $c_M/c_m = 1$ .

$$\frac{l_d}{d_b} = \frac{\frac{f_y}{f_c'^{1/4}} - 2130}{80.2 \left( \frac{c + K_{tr}}{d_b} \right)} \quad (14)$$

in which  $c = c_m + 0.5 d_b$  = smaller of the cover to the center of the bar or one-half of the center-

to-center bar spacing (Note: The simplification includes dropping 0.25 in. from the definition of  $c_s$  that follows Eq. 1)

$$K_{tr} = K_{tr}(\text{conv.}) = 34.5 (0.72 d_b + 0.28) \frac{A_{tr}}{sn} \text{ for conventional reinforcement (average } R_f = 0.0727)$$

$$K_{tr} = K_{tr}(\text{new}) = 53 (0.72 d_b + 0.28) \frac{A_{tr}}{sn} \text{ for new reinforcement (average } R_f = 0.1275)$$

The term  $(c + K_{tr})/d_b$  in Eq. 14 must be limited to a maximum value of 4 to insure that a splitting failure, rather than a pullout failure, will govern bond strength. Values of  $(c + K_{tr})/d_b > 4$  do not provide an increase in strength commensurate with that predicted in Eq. 11 (Darwin et al. 1995).

The relative effect of high bearing area bars on development length can be evaluated using Eq. 14 by taking the ratio of  $l_d$  for the new reinforcement to  $l_d$  for conventional bars.

$$\frac{l_d(\text{new})}{l_d(\text{conv.})} = \frac{c + K_{tr}(\text{conv.})}{c + K_{tr}(\text{new})} \quad (15)$$

The maximum reduction in  $l_d$  will occur for  $c/d_b = 1$  [the minimum allowed under the ACI Building Code (1989)] and  $[c + K_{tr}(\text{new})]/d_b = 4$ . In this case,  $K_{tr}(\text{new})/d_b = 3$  and  $K_{tr}(\text{conv.})/d_b = (34.5/53) 3 = 0.65 \times 3 = 1.95$ , giving  $l_d(\text{new})/l_d(\text{conv.}) = 0.74$ , for a 26 percent savings. For  $c/d_b = 1$  and  $K_{tr}(\text{new})/d_b = 2$  and 1, the savings become 23 and 19 percent, respectively. Values of  $l_d(\text{new})/l_d(\text{conv.})$  are summarized in Table 5 for  $c/d_b = 1, 1.5, 2, 2.5$  and 3, and  $K_{tr}(\text{new})/d_b = 0, 1, 2$  and 3. Table 5 demonstrates that lower savings will be obtained as cover and bar spacing increase, or when  $[c + K_{tr}(\text{new})]/d_b$  exceeds 4.

### Evaluation of Test Results – Epoxy-Coated Bars

Bar stresses at failure for the ten splice specimens containing epoxy-coated high relative rib area bars [ $R_f = 0.10$  to 0.14] are compared to the corresponding uncoated bar specimens in Table 6. All of the splices had a cover of less than  $3 d_b$ , and nine out of ten of the matched pairs contained splices that were not confined by transverse reinforcement. The ratios of coated to uncoated bar splice strength, C/U, range from 0.82 to 0.95, with an overall average of 0.88. These values

contrast sharply with both 1) the average ratio of 0.66 for the 21 tests (Treece and Jirsa 1987, 1989) used to establish the current development length modification factor of 1.5 for bars with cover less than  $3 d_b$  or clear spacing less than  $6 d_b$  (ACI 318-89, AASHTO Highway 1992), and 2) the average ratio of 0.74, for a data base including 113 splice tests (Hester, Salamizavaregh, Darwin, and McCabe 1991, 1993). These comparisons indicate that high relative rib area bars will require lower development length modification factors than are in current use (ACI 318-89, AASHTO Highway 1992).

The size of the current data set, ten matched pairs of splice specimens, closely matches the 21 beams used to establish the current development length criteria. However, since 20 tests represent a relatively small data base and since additional tests are under way, it would seem wise to delay the formulation of specific recommendations for development length modification factors at this time. If the additional tests bare out the results presented in Table 6, the maximum development length modification factor for epoxy-coated bars could be dropped from 1.5 to 1.2, providing a 20 percent reduction in development and splice length. That reduction would apply whether or not the bars were confined by transverse reinforcement.

## SUMMARY AND CONCLUSIONS

This report describes the testing and analysis of 83 beam-splice specimens containing No. 5, No. 8, and No. 11 (16, 25, and 36 mm) bars with relative rib areas ranging from 0.065 to 0.140. Concretes containing two different coarse aggregates were used to evaluate the effect of aggregate properties on bond strength. Sixty specimens contained uncoated bars with confining transverse reinforcement. Thirteen specimens contained uncoated bars without confining reinforcement, and ten specimens contained epoxy-coated bars, nine without confining reinforcement and one with confining reinforcement. The tests were analyzed to determine the effect of relative rib area and bar diameter on the increase in bond strength provided by confining reinforcement. The tests also provided a preliminary indication of the effect of high relative rib area on the splice

strength of epoxy-coated bars.

The following conclusions are based on the test results and analyses presented in this report.

1. In the range of relative rib areas tested, the splice strength of uncoated bars not confined by transverse reinforcement does not appear to be affected by bar deformation pattern.
2. The splice strength of uncoated reinforcement confined by transverse reinforcement increases with an increase in the relative rib area of the spliced bars.
3. The splice strength of uncoated reinforcement confined by transverse reinforcement increases with an increase in the bar diameter of the spliced bars.
4. The increase in splice strength provided by transverse reinforcement is influenced by the properties of the coarse aggregate used in the concrete. For a given concrete compressive strength, higher strength coarse aggregates provide higher bond strengths.
5. The use of reinforcing bars with an average relative rib area  $R_r = 0.1275$  (minimum  $R_r = 0.12$ ) can provide up to a 26 percent decrease in splice length compared to conventional reinforcement. The savings obtainable with the high relative rib area bars is highest for low covers and bar spacings and high amounts of confining transverse reinforcement. The reduction in splice length decreases with increases in cover and bar spacing and decreases in transverse reinforcement. The relative savings with high  $R_r$  bars will also decrease for high levels of confinement that result in bar pullout rather than concrete splitting governing bond strength.
6. Epoxy coating appears to have a less detrimental effect on splice strength for high relative rib area bars than for conventional bars. The relative improvement in the splice strength of epoxy-coated reinforcement with an increase in  $R_r$  is obtained whether or not the splices are confined by transverse reinforcement. The results indicate that the maximum development length modification factor used for epoxy-coated reinforcement could be reduced as much as 20 percent compared to the current requirement.

## REFERENCES

AASHTO Highway Sub-Committee on Bridges and Structures. 1992. *Standard Specifications for Highway Bridges*, 15th Edition, American Association of State Highway and Transportation Officials, Washington, DC, 686 pp.

ACI Committee 318. 1989. *Building Code Requirements for Reinforced Concrete (ACI 318-89) and Commentary – ACI 318R-89*, American Concrete Institute, Detroit, MI, 353 pp.

ASTM. "Standard Specification for Deformed and Plain Billet-Steel Bars for Concrete Reinforcement. (ASTM A 615/A 615M-94)," *1995 Annual Book of ASTM Standards*, Vol. 1.04, American Society of Testing and Materials, Philadelphia, PA, pp. 300-304.

Azizinamini, A; Stark, M.; Roller, John J.; and Ghosh, S. K. 1993. "Bond Performance of Reinforcing Bars Embedded in High-Strength Concrete," *ACI Structural Journal*, Vol. 95, No. 5, Sept.-Oct., pp. 554-561.

Azizinamini, A; Chisala, M.; and Ghosh, S. K. 1995. "Tension Development Length of Reinforcing Bars Embedded in High-Strength Concrete," *Engineering Structures*, in press.

Chamberlin, S. J. 1956. "Spacing of Reinforcement in Beams," *ACI Journal, Proceedings* Vol. 53, No. 1, July, pp. 113-134.

Chamberlin, S. J. 1958. "Spacing of Spliced Bars in Beams," *ACI Journal, Proceedings* Vol. 54, No. 8, Feb., pp.689-698.

Chinn, James; Ferguson, Phil M.; and Thompson, J. Neils 1955. "Lapped Splices in Reinforced Concrete Beams," *ACI Journal, Proceedings*, Vol. 52, No. 2, Oct., pp. 201-214.

Choi, Oan Chul; Hadje-Ghaffari, Hossain; Darwin, David; and McCabe Steven L. 1990. "Bond of Epoxy-Coated Reinforcement to Concrete: Bar Parameters," *SL Report* No. 90-1, University of Kansas Center for Research, Lawrence, Kansas, Jan., 43 pp.

Choi, Oan Chul; Hadje-Ghaffari, Hossain; Darwin, David; and McCabe Steven L. 1991. "Bond of Epoxy-Coated Reinforcement: Bar Parameters," *ACI Materials Journal*, Vol. 88, No. 2, March-April, pp. 207-217.

Darwin, D.; McCabe, S. L.; Idun, E. K.; and Schoenekase, S. P. 1992a. "Development Length Criteria: Bars without Transverse Reinforcement," *SL Report* 92-1, University of Kansas Center for Research, Lawrence, Kansas, Apr., 62 pp.

Darwin, D.; McCabe, S. L.; Idun, E. K.; and Schoenekase, S. P. 1992b. "Development Length Criteria: Bars Not Confined by Transverse Reinforcement," *ACI Structural Journal*, Vol. 89, No. 6, Nov.-Dec., pp. 709-720.

Darwin, D. and Graham, E. K. 1993a. "Effect of Deformation Height and Spacing on Bond Strength of Reinforcing Bars," *SL Report* 93-1, University of Kansas Center for Research, Lawrence, Kansas, Jan., 68 pp.

Darwin, D. and Graham, E. K. 1993b. "Effect of Deformation Height and Spacing on Bond Strength of Reinforcing Bars," *ACI Structural Journal*, Nov.-Dec., Vol. 90, No. 6, pp. 646-657.



- Darwin, D.; Zuo, Jun; Tholen, Michael L.; and Idun, Emmanuel K. 1995. "Development Length Criteria for Conventional and High Relative Rib Area Reinforcing Bars," *SL Report 95-4*, University of Kansas Center for Research, Lawrence, Kansas, May, in press.
- DeVries, R. A.; Moehle, J. P.; and Hester, W. 1991. "Lap Splice Strength of Plain and Epoxy-Coated Reinforcement," *Report No. UCB/SEMM-91/02*, University of California, Berkeley, California, Jan., 86 pp.
- Ferguson, Phil M. and Thompson, J. Neils. 1965. "Development Length of High Strength Reinforcing Bars," *ACI Journal, Proceedings*, Vol. 62, No. 1, Jan., pp. 71-94.
- Ferguson, Phil M. and Breen, John E. 1965. "Lapped Splices for High Strength Reinforcing Bars," *ACI Journal, Proceedings*, Vol. 62, No. 9, Sept., pp. 1063-1078.
- Hester, Cynthia J.; Salamizavaregh, Shahin; Darwin, David; and McCabe, Steven L. 1991. "Bond of Epoxy-Coated Reinforcement to Concrete: Splices," *SL Report 91-1*, University of Kansas Center for Research, Lawrence, Kansas, May, 66 pp.
- Hester, Cynthia J.; Salamizavaregh, Shahin; Darwin, David; and McCabe, Steven L. 1993. "Bond of Epoxy-Coated Reinforcement: Splices," *ACI Structural Journal*, Vol. 90, No. 1, Jan.-Feb., pp. 89-102.
- Maeda, M.; Otani, S.; and Aoyama, H. 1991. "Bond Splitting Strength in Reinforced Concrete Members," *Transactions of the Japan Concrete Inst.*, Vol. 13, pp. 581-588.
- Mathey, Robert and Watstein, David. 1961. "Investigation of Bond in Beam and Pull-Out Specimens with High-Yield-Strength Deformed Bars," *ACI Journal, Proceedings*, Vol. 32, No. 9, Mar., pp. 1071-1090.
- Rezanoff, T.; Konkankar, U. S.; and Fu, Y. C. 1991. "Confinement Limits for Tension Lap Splices under Static Loading", *Report*, University of Saskatoon, Sask., Aug.
- Rezanoff, T.; Akanni, A; and Sparling, B. 1993. "Tensile Lap Splices under Static Loading: A Review of The Proposed ACI 318 Code Provisions," *ACI Structural Journal*, Vol. 90, No. 4, July-Aug., pp. 374-384.
- Sakurada, T; Morohashi, N.; and Tanaka, R. 1993. "Effect of Transverse Reinforcement on Bond Splitting Strength of Lap Splices," *Transactions of the Japan Concrete Inst.*, Vol. 15, pp. 573-580.
- Thompson, M. A.; Jirsa, J. O.; Breen, J. E.; and Meinheit, D. F. 1975. "The Behavior of Multiple Lap Splices in Wide Sections," *Research Report No. 154-1*, Center for Highway Research, The University of Texas at Austin, Feb., 75 pp.
- Treece, Robert A. and Jirsa, James O. 1987. "Bond Strength of Epoxy-Coated Reinforcing Bars," *PMFSEL Report No. 87-1*, Phil M. Ferguson Structural Engineering Laboratory, Univ. of Texas at Austin, Jan., 85 pp.
- Treece, Robert A. and Jirsa, James O. 1989. "Bond Strength of Epoxy-Coated Reinforcing Bars," *ACI Materials Journal*, Vol. 86, No. 2, Mar.-Apr., pp. 167-174.
- Zekany, A. J.; Neumann, S.; and Jirsa, J. O. 1981. "The Influence of Shear on Lapped Splices in Reinforced Concrete," *Research Report No. 242-2*, Center for Transportation Research, Bureau of Engineering Research, University of Texas at Austin, July, 88 pp.

**Table 1**  
**Splice specimen properties and test results**

Specimen No. +	Bar ++ Designation	n	$l_s$ (in.)	$d_b$ (in.)	$c_{so}$ (in.)	$c_{si}$ (in.)	$c_b$ (in.)	b (in.)	h (in.)	l (ft)	$l_c$ (ft)	d (in.)	$f'_c$ (psi)	N	$d_s$ (in.)	$f_{yt}$ (ksi)	P (kips)	$M_u$ (k-in.)	$f_s^{+++}$ (ksi)
1.1	8C1	2	16.0	1.000	2.969	2.938	2.938	16.08	17.22	13.00	4.00	13.76	5020				20.69	1021	51.63
1.2	8C1	2*	16.0	1.000	2.032	2.281	1.938	24.06	16.25	13.00	4.00	13.79	5020				35.53	1746	44.60
1.3	8C1	3	16.0	1.000	2.032	1.438	1.938	16.07	16.21	13.00	4.00	13.75	5020				26.74	1310	45.01
1.4	8C1**	3	16.0	1.000	2.032	1.375	1.938	16.11	16.20	13.00	4.00	13.74	5020				21.93	1079	37.09
1.5	8C1	3	16.0	1.000	2.063	1.375	1.938	16.07	16.19	13.00	4.00	13.74	5020	5	0.500	70.75	31.08	1518	52.22
1.6	8C1	3	16.0	1.000	2.063	1.438	1.938	16.05	16.19	13.00	4.00	13.74	5020	3	0.500	70.75	30.93	1511	51.98
2.1	8S0	2	24.0	1.000	2.250	1.706	1.328	12.12	15.56	16.00	6.00	13.70	5250	7	0.375	69.92	22.12	1214	62.43
2.2	8F1	2	24.0	1.000	2.125	1.801	1.406	12.12	15.52	16.00	6.00	13.58	5250	7	0.375	69.92	27.90	1526	77.60
2.3	8F1	2	24.0	1.000	2.125	1.780	1.969	12.11	16.06	16.00	6.00	13.56	5250	4	0.375	69.92	25.77	1413	73.45
2.4	8F1	2	24.0	1.000	2.000	1.914	1.313	12.13	15.64	16.00	6.00	13.79	5250				19.24	1059	54.08
2.5	8F1	2	24.0	1.000	2.063	1.856	1.813	12.13	16.01	16.00	6.00	13.67	5250				20.69	1138	58.67
2.6	8F1**	2	24.0	1.000	2.000	1.917	1.938	12.12	16.19	16.00	6.00	13.71	5250				17.41	961	49.37
3.4	8C0	2	24.0	1.000	2.110	1.857	2.000	12.14	16.26	16.00	6.00	13.73	5110	4	0.375	69.92	19.73	1087	55.77
3.5	8C0	3	28.0	1.000	1.001	0.965	1.906	12.17	16.17	16.00	6.00	13.74	3810	8	0.375	69.92	27.00	1479	52.02
4.1	8S0	2	24.0	1.000	2.063	1.926	1.250	12.16	15.49	16.00	6.00	13.72	4090	6	0.500	70.75	22.05	1211	62.51
4.2	8F1	2	24.0	1.000	2.094	1.848	1.313	12.17	15.59	16.00	6.00	13.74	4090	8	0.375	69.92	25.61	1403	72.33
4.4	8C1	2	24.0	1.000	2.032	1.978	1.219	12.15	15.47	16.00	6.00	13.73	4090	4	0.375	69.92	20.75	1141	58.85
4.5	8C1	2	24.0	1.000	2.063	1.936	1.844	12.12	16.15	16.00	6.00	13.79	4090				18.02	994	51.06
4.6	8C1**	2	24.0	1.000	2.094	1.926	2.000	12.16	16.23	16.00	6.00	13.72	4090				14.57	808	41.72
5.1	8SH0	3	24.0	1.000	2.016	1.914	1.250	18.22	15.57	16.00	6.00	13.79	4190	7	0.375	69.92	34.41	1888	64.61
5.2	8F1	3	24.0	1.000	2.078	1.867	1.359	18.12	15.62	16.00	6.00	13.73	4190	7	0.375	69.92	34.67	1902	65.42
5.3	8F1	2	24.0	1.000	2.063	1.849	1.281	12.11	15.50	16.00	6.00	13.68	4190	7	0.375	69.92	23.90	1311	67.86
5.4	8SH0	2	24.0	1.000	1.985	1.980	1.250	12.12	15.46	16.00	6.00	13.68	4190	7	0.375	69.92	20.69	1137	58.88
5.5	8C0	2	24.0	1.000	2.063	1.904	1.406	12.12	15.60	16.00	6.00	13.67	4190	4	0.375	69.92	16.22	896	46.42
5.6	8F1	2	22.0	1.000	2.094	1.807	1.313	12.11	15.69	16.00	6.00	13.84	4190	5	0.500	70.75	23.65	1297	66.36
6.1	8SH0	3	24.0	1.000	2.063	0.422	1.906	12.18	16.12	16.00	6.00	13.69	4220	8	0.500	66.42	32.89	1797	63.24
6.2	8F1	3	24.0	1.000	2.000	0.438	2.000	12.11	16.15	16.00	6.00	13.62	4220	8	0.500	66.42	38.79	2115	74.92
6.3	8F1	2	16.0	1.000	2.000	1.906	1.344	12.13	15.51	16.00	6.00	13.63	4220	2	0.375	64.55	16.07	887	46.09
6.4	8C0	2	16.0	1.000	2.094	1.844	1.344	12.11	15.45	16.00	6.00	13.58	4220	2	0.375	64.55	12.67	703	36.68
6.5	8F1	2	24.0	1.000	2.000	1.906	1.969	12.10	16.13	16.00	6.00	13.63	4220				18.71	1031	53.59
6.6	8F1**	2	24.0	1.000	2.032	1.875	1.969	12.15	16.13	16.00	6.00	13.63	4220				17.30	955	49.63
7.1	8F1	2	16.0	1.000	2.079	1.797	1.875	12.00	16.18	16.00	6.00	13.77	4160	2	0.375	64.55	15.56	908	46.72
7.2	8C1	2	18.0	1.000	1.469	2.531	1.313	12.06	15.54	16.00	6.00	13.72	4160	5	0.500	84.70	18.81	1081	55.82
7.5	8F1	3	24.0	1.000	2.032	0.399	2.000	11.97	16.17	16.00	6.00	13.64	4160	8	0.500	84.70	37.07	2068	73.17
7.6	8C1	2	16.0	1.000	2.032	1.969	1.938	12.01	16.22	16.00	6.00	13.77	4160	2	0.375	64.55	14.70	862	44.34
8.1	8N0	3	24.0	1.000	2.032	0.453	1.953	12.13	16.23	16.00	6.00	13.76	3830	8	0.500	84.70	36.34	1983	69.67
8.2	8N3	3	24.0	1.000	2.047	0.430	1.969	12.16	16.20	16.00	6.00	13.69	3830	8	0.500	84.70	41.23	2247	79.32
8.3	8N0	2	24.0	1.000	2.000	1.953	2.000	12.11	16.05	16.00	6.00	13.53	3830				21.30	1171	61.47

**Table 1**  
**Splice specimen properties and test results (continued)**

Specimen No. +	Bar ++ Designation	n	$l_s$ (in.)	$d_b$ (in.)	$c_{s0}$ (in.)	$c_{s1}$ (in.)	$c_b$ (in.)	b (in.)	h (in.)	l (ft)	$l_c$ (ft)	d (in.)	$f'_c$ (psi)	N	$d_s$ (in.)	$f_{yt}$ (ksi)	P (kips)	$M_u$ (k-in.)	$f_s$ +++ (ksi)
8.4	8N3	2	16.0	1.000	2.063	1.891	1.906	12.10	16.35	16.00	6.00	13.91	3830	2	0.375	64.55	17.38	959	48.90
9.1	8N3	2	24.0	1.000	2.032	1.875	1.954	12.14	16.19	16.00	6.00	13.70	4230	2	0.375	64.55	22.33	1226	63.40
9.2	8F1	2	18.0	1.000	2.063	1.844	1.290	12.10	15.67	16.00	6.00	13.84	4230	6	0.375	64.55	24.65	1351	69.06
9.3	8N0	2	24.0	1.000	2.094	1.907	1.818	12.19	16.12	16.00	6.00	13.78	4230	2	0.375	64.55	19.54	1076	55.25
9.4	8F1	2	24.0	1.000	2.016	1.891	1.915	12.11	16.17	16.00	6.00	13.72	4230	2	0.375	64.55	22.94	1259	65.00
10.1	8N3**	2	26.0	1.000	2.016	1.907	1.896	12.15	16.16	16.00	6.00	13.72	4250				20.36	1120	57.79
10.2	8N3	2	26.0	1.000	2.063	1.875	1.933	12.13	16.25	16.00	6.00	13.78	4250				21.66	1191	61.17
10.3	8N0	2	26.0	1.000	2.094	1.844	1.798	12.11	16.09	16.00	6.00	13.77	4250	2	0.375	64.55	20.81	1144	58.85
10.4	8N0	2	20.0	1.000	2.079	1.875	1.916	12.07	16.19	16.00	6.00	13.75	4250	5	0.500	84.70	21.91	1204	61.98
11.1	8F1	3	18.0	1.000	2.000	0.453	1.928	12.20	16.14	16.00	6.00	13.68	4380	6	0.500	84.70	34.85	1902	66.94
11.2	8N0	2	18.0	1.000	2.094	1.844	1.881	12.19	16.13	16.00	6.00	13.72	4380	4	0.500	84.70	21.88	1202	61.94
11.3	8N3	2	18.0	1.000	2.063	1.844	1.943	12.13	16.08	16.00	6.00	13.60	4380	4	0.500	84.70	21.85	1200	62.44
11.4	8F1	2	24.0	1.000	2.094	1.844	1.928	12.15	16.23	16.00	6.00	13.77	4380	2	0.375	64.55	22.14	1217	62.49
12.1	5N0	4	10.0	0.625	1.875	0.521	1.335	12.07	15.56	13.00	4.00	13.90	4120	2	0.500	84.70	14.34	708	45.42
12.2	5C2	4	10.0	0.625	1.953	0.516	1.297	12.12	15.57	13.00	4.00	13.94	4120	2	0.500	84.70	14.40	711	45.48
12.3	5N0	3	10.0	0.625	2.032	1.039	1.291	12.14	15.50	13.00	4.00	13.88	4120	1	0.375	64.55	11.54	573	48.52
12.4	5C2	3	10.0	0.625	2.063	1.032	1.264	12.12	15.56	13.00	4.00	13.96	4120	1	0.375	64.55	12.48	618	52.02
13.1	5C2	3	12.0	0.625	1.532	1.289	1.303	12.18	15.51	13.00	4.00	13.88	4110	1	0.375	64.55	13.33	659	55.82
13.2	5N0	3	12.0	0.625	1.563	1.266	1.315	12.11	15.50	13.00	4.00	13.86	4110	1	0.375	64.55	13.38	661	56.10
13.3	5C2**	3	16.0	0.625	2.047	1.000	1.325	12.15	15.52	13.00	4.00	13.86	4110				12.84	636	53.91
13.4	5C2	3	16.0	0.625	2.094	1.016	1.354	12.19	15.60	13.00	4.00	13.92	4110				14.38	710	59.96
14.1	8C1	3	36.0	1.000	2.032	0.484	1.877	12.12	16.26	16.00	6.00	13.86	4200	3	0.375	64.55	31.53	1725	59.96
14.2	8C1	3	21.0	1.000	2.016	0.469	1.897	12.19	16.13	16.00	6.00	13.72	4200	7	0.500	84.70	32.73	1788	62.83
14.3	5C2	3	17.0	0.625	2.032	1.031	1.295	12.14	15.51	13.00	4.00	13.89	4200				15.06	743	62.84
14.4	5C2**	3	17.0	0.625	2.063	1.000	1.320	12.14	15.59	13.00	4.00	13.94	4200				13.76	680	57.34
14.5	5N0	2	12.0	0.625	1.594	3.156	1.210	12.13	15.45	13.00	4.00	13.91	4200	2	0.375	64.55	9.64	482	60.15
14.6	5C2	2	12.0	0.625	1.532	3.188	1.277	12.05	15.49	13.00	4.00	13.89	4200	2	0.375	64.55	10.17	507	63.45
15.1	11F3	2	27.0	1.410	1.516	1.500	1.902	12.11	16.11	16.00	6.00	13.46	5250	9	0.500	84.70	44.97	2449	67.33
15.2	11N0	2	27.0	1.410	1.610	1.469	1.924	12.11	16.12	16.00	6.00	13.46	5250	9	0.500	84.70	41.96	2287	62.89
15.3	11N0	2	40.0	1.410	1.516	1.531	1.820	12.04	16.19	16.00	6.00	13.63	5250	10	0.375	64.55	41.92	2287	62.07
15.4	11F3	2	40.0	1.410	1.563	1.469	1.884	12.08	16.13	16.00	6.00	13.50	5250	10	0.375	64.55	51.57	2808	76.93
15.5	11F3	2	40.0	1.410	3.063	2.984	1.908	18.05	16.12	16.00	6.00	13.47	5250				36.65	2013	54.12
15.6	11F3**	2	40.0	1.410	2.922	3.063	1.932	18.07	16.10	16.00	6.00	13.42	5250				32.45	1787	48.19
16.1	11F3**	2	40.0	1.410	3.063	2.906	1.833	18.04	15.93	16.00	6.00	13.35	5180				32.68	1799	48.83
16.2	11F3	2	40.0	1.410	3.016	2.969	1.895	18.07	16.28	16.00	6.00	13.64	5180				35.92	1974	52.38
16.3	11F3	2	40.0	1.410	3.047	2.969	1.791	18.03	16.16	16.00	6.00	13.62	5180	4	0.375	64.55	42.18	2312	61.42
16.4	11B0	2	40.0	1.410	3.063	3.000	1.846	18.06	16.00	16.00	6.00	13.45	5180	4	0.375	64.55	41.45	2272	61.19

**Table 1**  
**Splice specimen properties and test results (continued)**

Specimen No. +	Bar ++ Designation	n	$l_g$ (in.)	$d_b$ (in.)	$c_{s0}$ (in.)	$c_{si}$ (in.)	$c_b$ (in.)	b (in.)	h (in.)	l (ft)	$l_c$ (ft)	d (in.)	$f'_c$ (psi)	N	$d_s$ (in.)	$f_{yt}$ (ksi)	P (kips)	$M_u$ (k-in.)	$f_s$ +++ (ksi)
17.3	11F3	2	38.0	1.410	3.047	2.984	1.888	18.03	16.12	16.00	6.00	13.48	4710	8	0.375	64.55	46.74	2558	68.85
17.4	11B0	2	38.0	1.410	3.094	3.000	1.866	18.07	16.09	16.00	6.00	13.49	4710	8	0.375	64.55	44.77	2451	65.98
17.5	11B0	2	30.0	1.410	3.079	3.000	1.907	18.09	16.09	16.00	6.00	13.45	4710	7	0.500	84.70	39.69	2175	58.72
17.6	11F3	2	30.0	1.410	3.063	2.969	1.911	18.07	16.20	16.00	6.00	13.54	4710	7	0.500	84.70	47.03	2572	68.92
18.1	11F3	2	40.0	1.410	1.484	4.500	1.845	18.05	16.11	16.00	6.00	13.52	4700	10	0.375	64.55	55.06	3007	80.72
18.2	11F3**	2	40.0	1.410	2.984	3.000	1.922	18.07	16.14	16.00	6.00	13.48	4700	6	0.375	68.90	38.88	2134	57.48
18.3	11F3	2	40.0	1.410	3.031	3.000	1.911	18.05	16.08	16.00	6.00	13.43	4700	6	0.375	64.55	46.85	2564	69.33
18.4	11B0	2	40.0	1.410	3.016	3.031	1.871	18.08	16.23	16.00	6.00	13.62	4700	6	0.375	64.55	45.49	2491	66.33

+ Specimen No.  
G.P, G = group number (1-18), P = casting order in the group (1-6)

++ Bar Designation  
#AA, # = bar size (No. 5, No. 8 or No. 11), AA = bar manufacturer and deformation pattern

B0	Conventional Birmingham Steel bar	N0	Conventional North Star Steel bar
C0	Conventional Chaparral Steel bar	N3	New North Star Steel bar
C1, C2	New Chaparral Steel bars	S0	Conventional Structural Metals, Inc. bar
F1, F3	New Florida Steel bars	SH0	Conventional Sheffield Steel bar

+++ Bar stress is computed based on working stress if  $f_s$  does not exceed bar yield stress, otherwise computed based on ultimate strength  
 $M_u$  and  $f_s$  include effects of beam self weight and loading system

\* Contained 2 splices and 2 continuous bars

\*\* Spliced bars were coated

1 in. = 25.4 mm; 1 ft = 305 mm; 1 psi = 6.89 kPa; 1 ksi = 6.89 MPa; 1 kip = 4.45 kN; 1 k-in. = 0.113 kN-m

**Table 2**  
**Properties of reinforcing bars**

Bar + Designation	Yield Str. (ksi)	Nominal Diameter (in.)	Weight (lb/ft)	% Light or Heavy	Rib Spacing (in.)	ASTM Rib Height (in.)	Avg. * Rib Height (in.)	Relative Rib Area	Coating Thick. ** (mils)
5N0	65.00	0.625	1.015	2.6% L	0.350	0.036	0.035	0.082	-
5C2	64.00	0.625	1.013	2.9% L	0.275	0.042	0.041	0.109	9.9
8C0		1.000	2.615	2.1% L	0.589	0.066	0.063	0.085	-
8C1	60.00	1.000	2.529	5.3% L	0.504	0.064	0.060	0.101	13.3
8F1	75.00	1.000	2.600	2.6% L	0.471	0.078	0.074	0.140	16.8
8N0	79.00	1.000	2.594	2.8% L	0.650	0.057	0.054	0.069	-
8N3	81.00	1.000	2.730	2.2% H	0.487	0.072	0.068	0.119	12.1
8S0	70.00	1.000	2.568	3.8% L	0.668	0.056	0.054	0.071	-
8SH0		1.000	2.618	1.9% L	0.637	0.054	0.052	0.065	-
11N0	64.00	1.410	5.157	2.9% L	0.911	0.079	0.075	0.072	-
11B0	70.00	1.410	5.102	4.0% L	0.825	0.070	0.066	0.070	-
11F3	81.00	1.410	5.145	3.2% L	0.615	0.090	0.088	0.127	6.3

+ Bar Designation  
#AA, # = bar size (No. 5, No. 8 or No. 11), AA = bar manufacturer and deformation pattern

B0 Conventional Birmingham Steel bar  
C0 Conventional Chaparral Steel bar  
C1, C2 New Chaparral Steel bars  
F1, F3 New Florida Steel bars  
N0 Conventional North Star Steel bar  
N3 New North Star Steel bar  
S0 Conventional Structural Metals, Inc. bar  
SH0 Conventional Sheffield Steel bar

- No coated bars tested

\* Average rib height between longitudinal ribs

\*\* Average coating thicknesses for epoxy-coated bars belonging to bar designation

1 ksi = 6.89 MPa; 1 in. = 25.4 mm; 1 lb/ft = 1.49 kg/m; 1 mil = 0.001 in. = 25.4  $\mu$ m

**Table 3**  
**Concrete mix proportions (lb/yd<sup>3</sup>) and properties**

Group	w/c Ratio	Cement	Water	Fine Agg.*	Coarse Agg. Type	wr	Slump	Concrete Temp	Air Content	Test Age	Cylinder Strength	
						(oz)	(in.)	(F)	(%)	(days)	(psi)	
1	0.41	550	225	1564	L	1588	0	2.00	80	3.50	14	5020
2	0.36	575	205	1556	L	1588	3	0.75	91.5	3.10	7	5250
3	0.36	575	205	1556	L	1588	3	2.75	93	3.70	5	3810
											7	5110
4	0.36	575	205	1556	L	1588	3	1.75	95	4.50	5	4090
5	0.36	575	205	1556	L	1588	3	1.00	83	3.60	5	4190
6	0.36	575	205	1556	L	1588	3	2.25	77	4.70	5	4220
7	0.36	575	205	1556	L	1588	3	5.25	67	3.50	7	4160
8	0.45	556	250	1556	B	1670	0	1.25	86	3.00	8	3830
9	0.45	578	260	1512	B	1670	0	3.00	95	2.30	16	4230
10	0.42	578	240	1512	B	1670	0	2.50	91	2.50	10	4250
11	0.42	578	240	1512	B	1670	0	3.00	91	2.10	7	4380
12	0.36	575	205	1556	L	1588	3	2.50	88	5.50	6	4120
13	0.36	575	205	1556	L	1588	3	2.50	91	5.20	6	4110
14	0.44	511	225	1564	L	1661	0	2.50	90	2.90	10	4200
15	0.44	511	225	1564	L	1661	0	2.50	83	2.30	19	5250
16	0.44	511	225	1564	L	1661	0	3.25	59	3.10	22	5180
17	0.44	511	225	1564	L	1661	0	2.50	59	4.00	21	4710
18	0.44	511	225	1564	L	1661	0	2.50	65	3.70	30	4700

\* Kansas River Sand - Lawrence Sand Co., Lawrence, KS  
 Bulk Specific Gravity (SSD) = 2.62; Absorption = 0.5 %; Fineness Modulus = 2.89

L Crushed Limestone - Fogel's Quarry, Ottawa, KS  
 Bulk Specific Gravity (SSD) = 2.58; Absorption = 2.7 %; Max. Size = 3/4 in.;  
 Unit Weight = 90.5 lb/cu. ft

B Basalt - Iron Mountain Trap Rock Company  
 Bulk Specific Gravity (SSD) = 2.64; Absorption = 0.44 %; Max. Size = 3/4 in.;  
 Unit Weight = 95.5 lb/cu. ft

wr Water Reducer per 100 lb Cement

1 lb/yd<sup>3</sup> = 0.5933 kg/m<sup>3</sup>; 1 oz = 29.57 cm<sup>3</sup>; 1 psi = 6.89 kPa

Table 4

Analysis of effects of relative rib area,  $R_r$ , and bar diameter,  $d_b$ , on increase in splice strength, represented by  $T_s/f'_c{}^{1/4}$ , provided by transverse reinforcement, represented by  $NA_{tr}/n$  ( $T_s$  in lb,  $f'_c$  in psi, and  $A_{tr}$  in in.<sup>2</sup>)

Bars	No. of Tests	Weighted Mean $R_r$	m+	b++	Mean+++ Slope, M	$M_{R_r = 0.075}^{+++}$	$t_r^*$	$M/t_r^{**}$
Conv. No. 5 (L)***	4	0.082	1347	100	1397	1348	1.036	1310
5C2 (L)	4	0.109	1524	122	1585		1.176	1196
Conv. No. 8 (L)	19	0.073	1727	-228	1612	1606	1.004	1643
8C1 (L)	7	0.101	1901	100	1951		1.214	1563
8F1 (L)	10	0.140	2594	84	2636		1.641	1625
Conv. No. 8 (B)	5	0.069	2415	-382	2224	2295	0.969	
8N3 (B)	4	0.119	3078	-36	3060		1.333	
8F1 (B)	4	0.140	3879	5	3881		1.691	
Conv. No. 11 (L)	6	0.071	1876	333	2043	2138	0.956	2134
11F3 (L)	7	0.127	2909	732	3275		1.532	2188

+Slope of best-fit line

++Intercept of best-fit line at  $NA_{tr}/n = 0$

+++ $M = (2m + b)/2$

+++Based on best-fit line for each bar size and concrete type

\* $t_r = M/M_{R_r = 0.075}$

\*\* $t_r = 9.6 R_r + 0.28$  (used to calculate  $t_d$ )

\*\*\*L = limestone coarse aggregate

B = basalt coarse aggregate

1 lb = 4.45 N; 1 psi = 6.89 kPa; 1 in. = 25.4 mm

Table 5

**Ratios of development lengths,  $l_d(\text{new})/l_d(\text{conv.})$ , comparing new (high  $R_r$ ) and conventional reinforcing bars confined by transverse reinforcement (based on Eq. 14)**

$c/d_b$	$K_{tr}(\text{new})/d_b^*$			
	0	1	2	3
1	1.00	0.83	0.77	0.74
1.5	1.00	0.86	0.80	0.86
2	1.00	0.88	0.83	0.99
2.5	1.00	0.90	0.95	1.00
3	1.00	0.91	1.00	1.00

$$*K_{tr}(\text{conv.}) = 0.65 K_{tr}(\text{new})$$

$$(c + K_{tr})/d_b \leq 4$$



Table 6

Comparison of splice strengths for epoxy-coated (C) and uncoated (U) high  $R_r$  bars

Bar Size	Bar Designation	$R_r^*$	Specimen No.	Surface Condition	Bar Stress (ksi)	$\frac{C}{U}^{**}$
No. 5	5C2	0.109	13.4	U	59.96	0.899
			13.3	C	53.91	
			14.3	U	62.84	
			14.4	C	57.34	
No. 8	8C1	0.101	1.3	U	45.01	0.824
			1.4	C	37.09	
			4.5	U	51.06	
			4.6	C	41.72	
	8N3	0.119	10.1	U	61.17	0.945
			10.2	C	57.79	
	8F1	0.140	2.5	U	58.67	0.841
			2.6	C	49.37	
			6.5	U	53.59	
			6.6	C	49.63	
No. 11	11F3	0.127	15.5	U	54.12	0.890
			15.6	C	48.19	
			16.2	U	52.38	
			16.1	C	48.83	
			18.3***	U	69.33	
			18.2***	C	57.48	
Average						0.882

\* $R_r$  = relative rib area

\*\*C/U = ratio of splice strengths of coated to uncoated bars

\*\*\*Splices confined by stirrups

1 ksi = 6.89 MPa

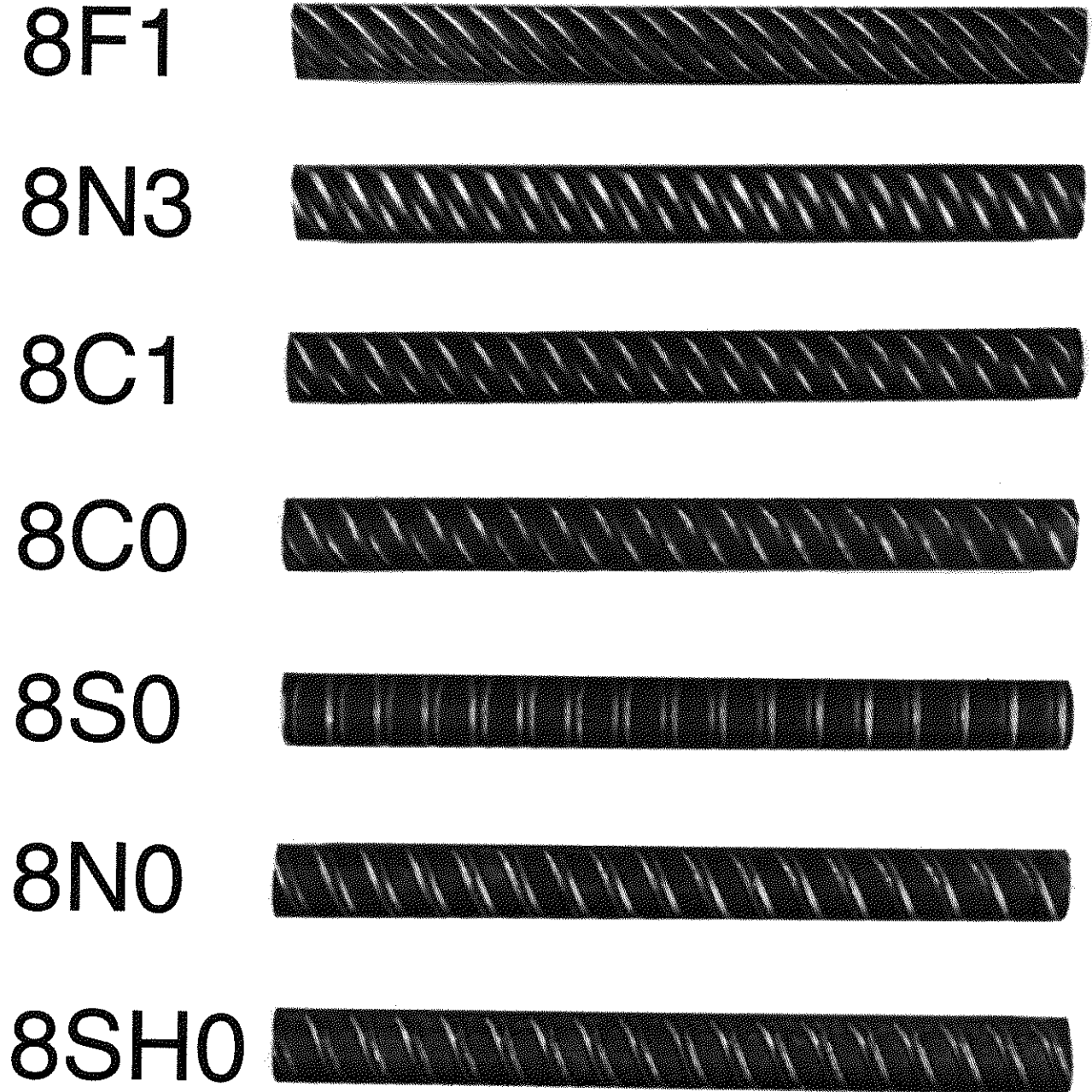


Fig. 1a Reinforcing bar deformation patterns, No. 8 (25 mm) bars

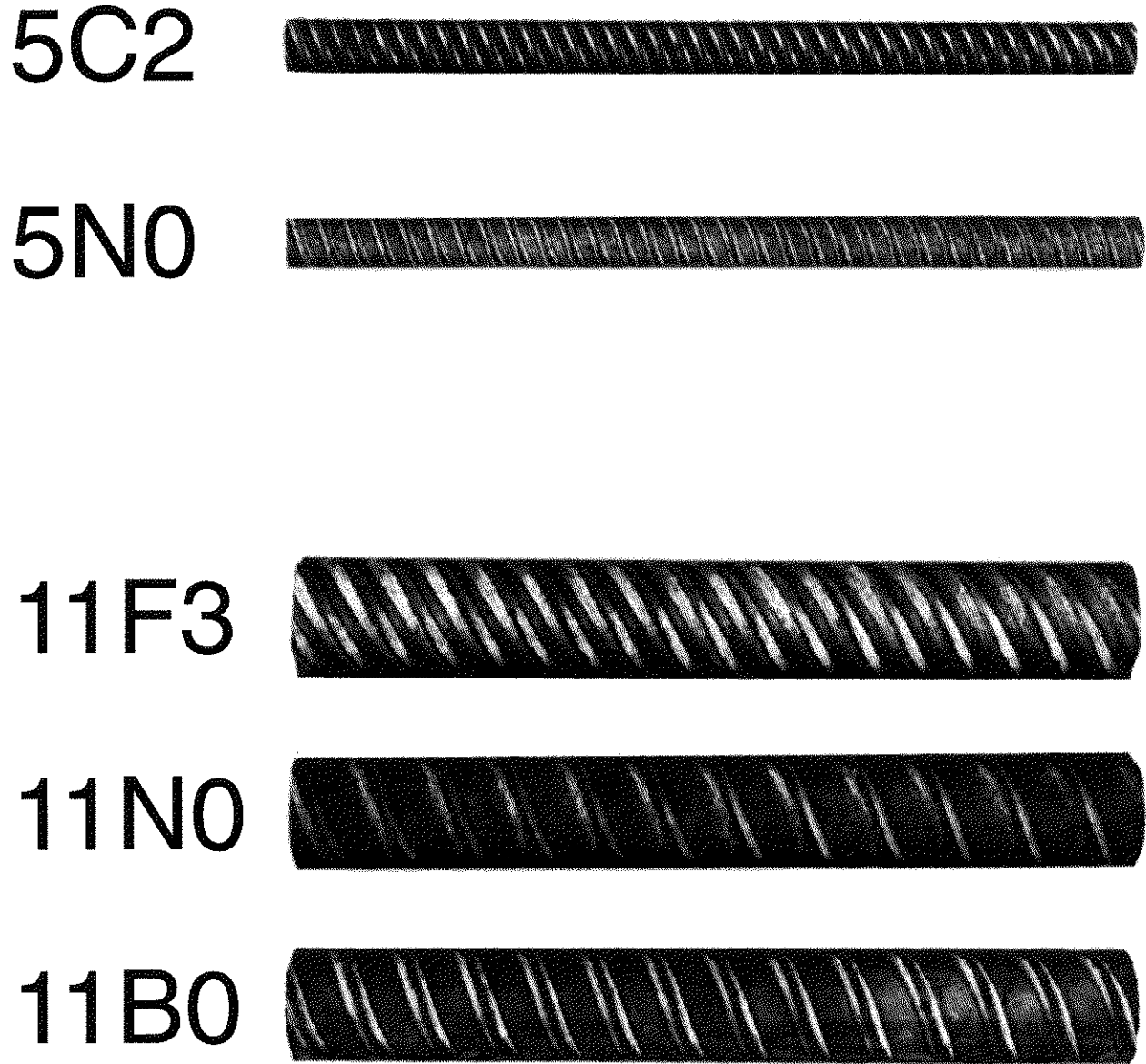


Fig. 1b Reinforcing bar deformation patterns, No. 5 and No. 11 (16 and 36 mm) bars

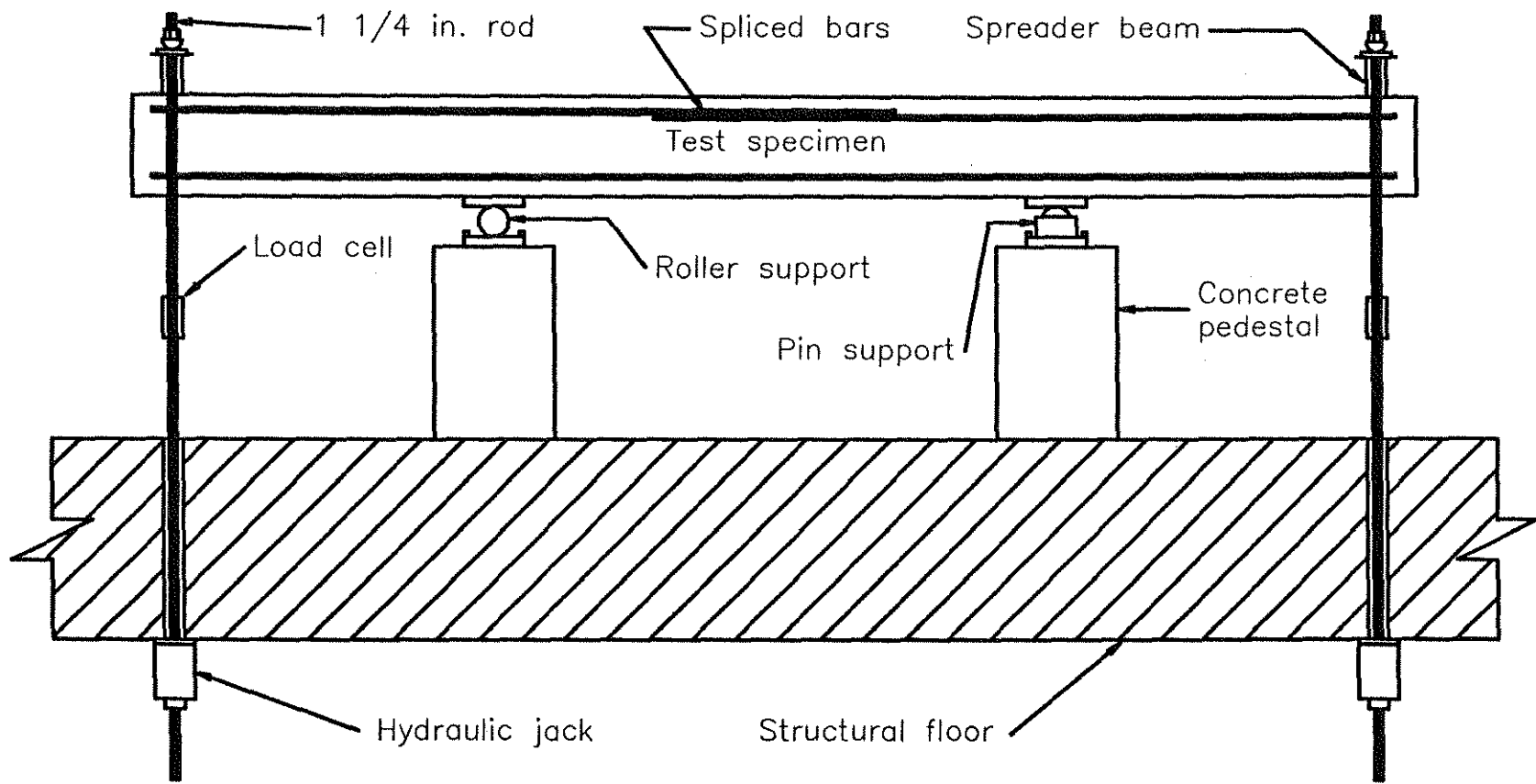


Fig. 2 Schematic of test apparatus

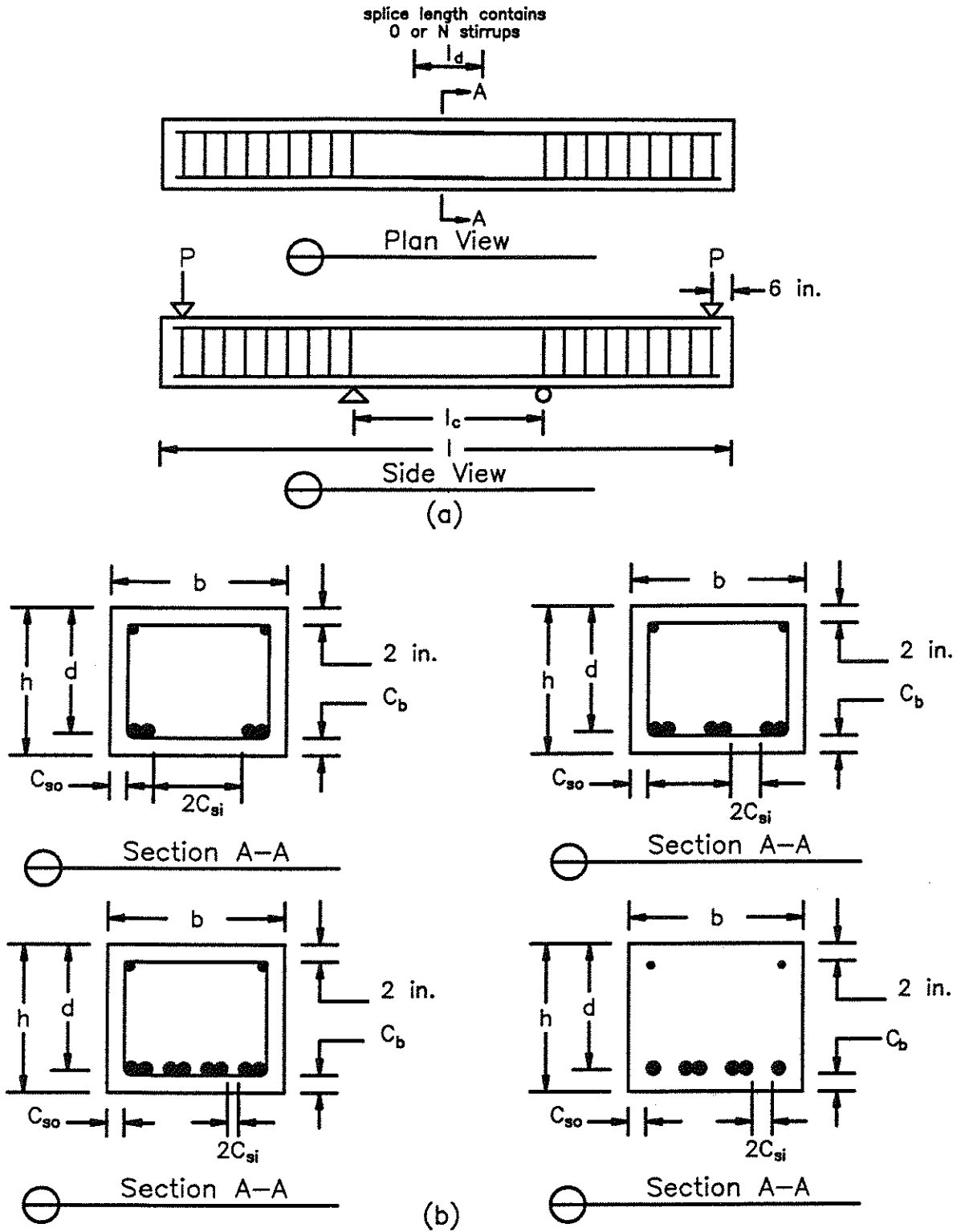
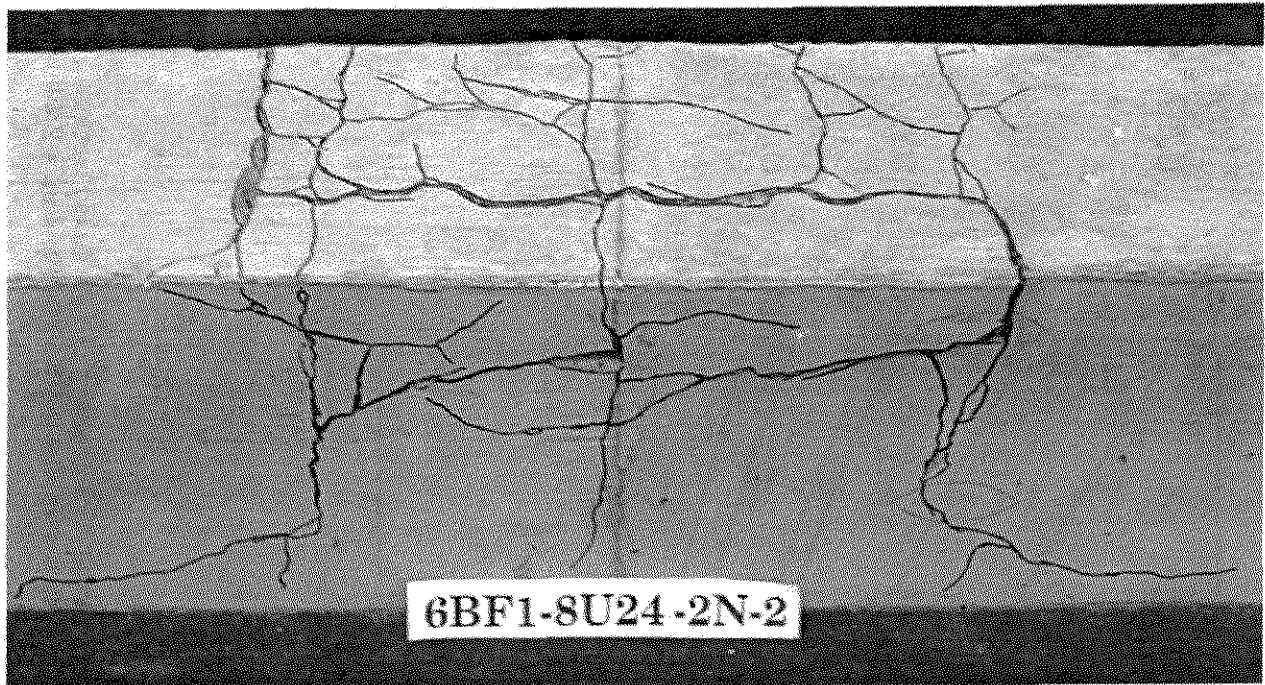
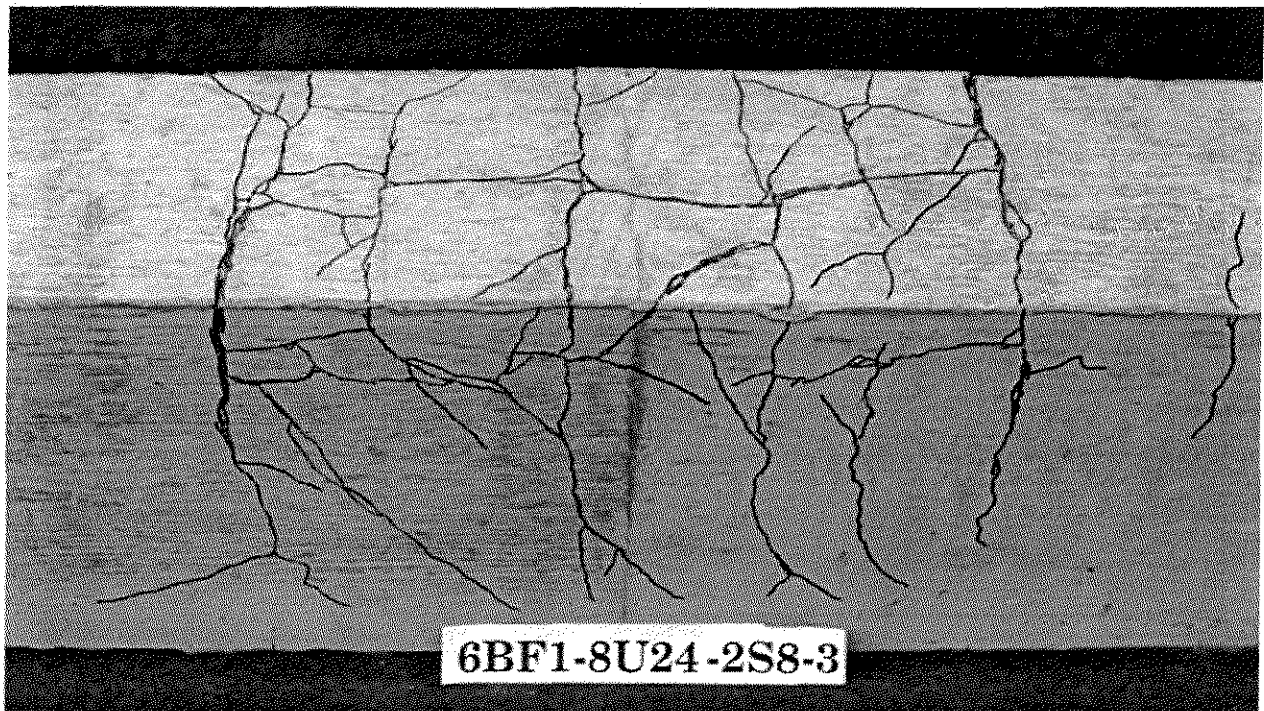


Fig. 3 Splice test specimens, (a) as tested, (b) configurations as cast (1 in. = 25.4 mm)



(a)



(b)

Fig. 4 Cracked splice specimens after failure, (a) without confining reinforcement, (b) with confining reinforcement

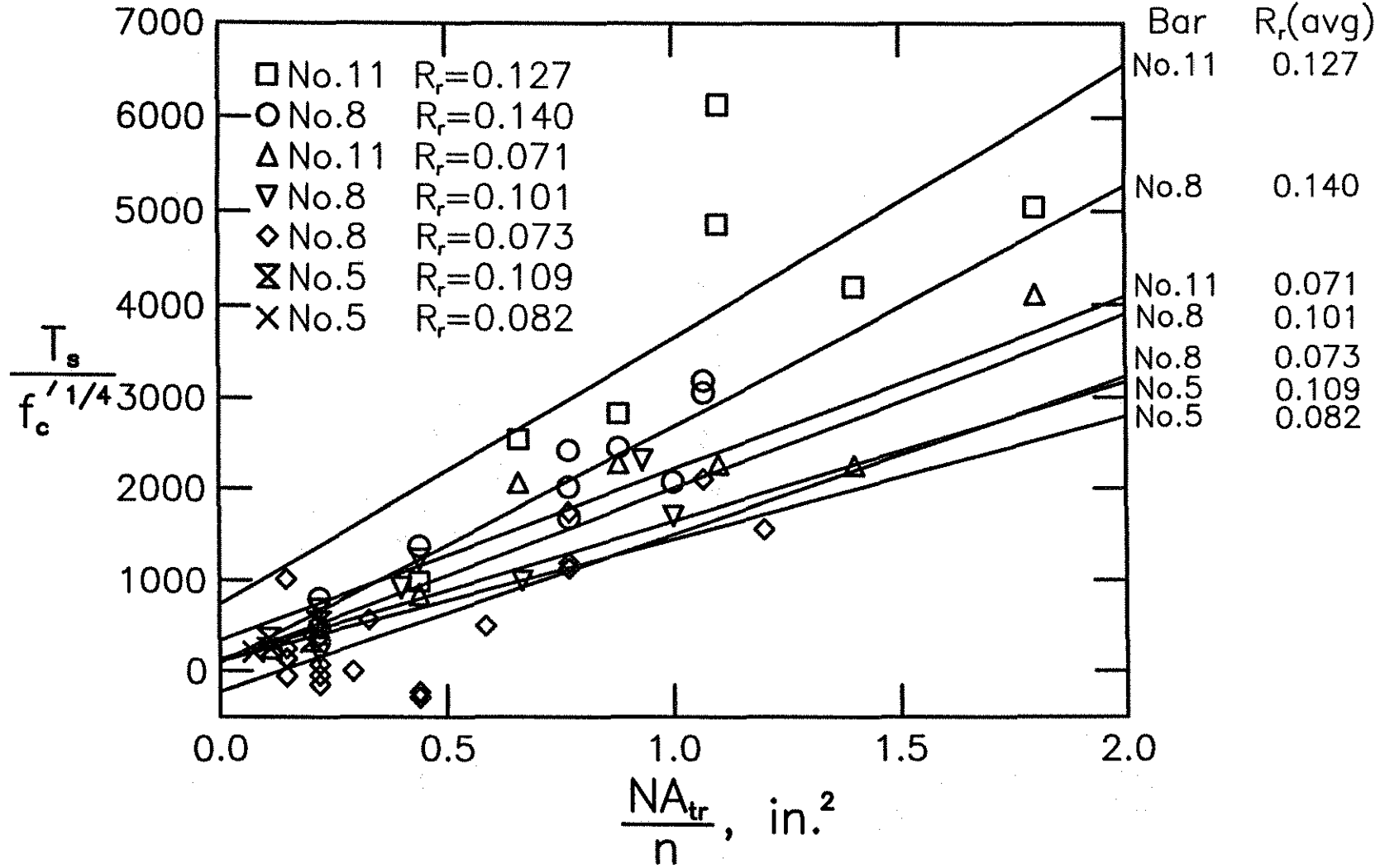


Fig. 5 Increase in bond force,  $T_s$ , normalized with respect to  $f_c^{1/4}$  versus effective transverse reinforcement  $NA_{tr}/n$ , for splices in concrete containing limestone coarse aggregate ( $T_s$  in lb,  $f_c$  in psi,  $A_{tr}$  in in.<sup>2</sup>) (1 lb = 4.45N, 1 psi = 6.89 kPa, 1 in. = 25.4 mm)

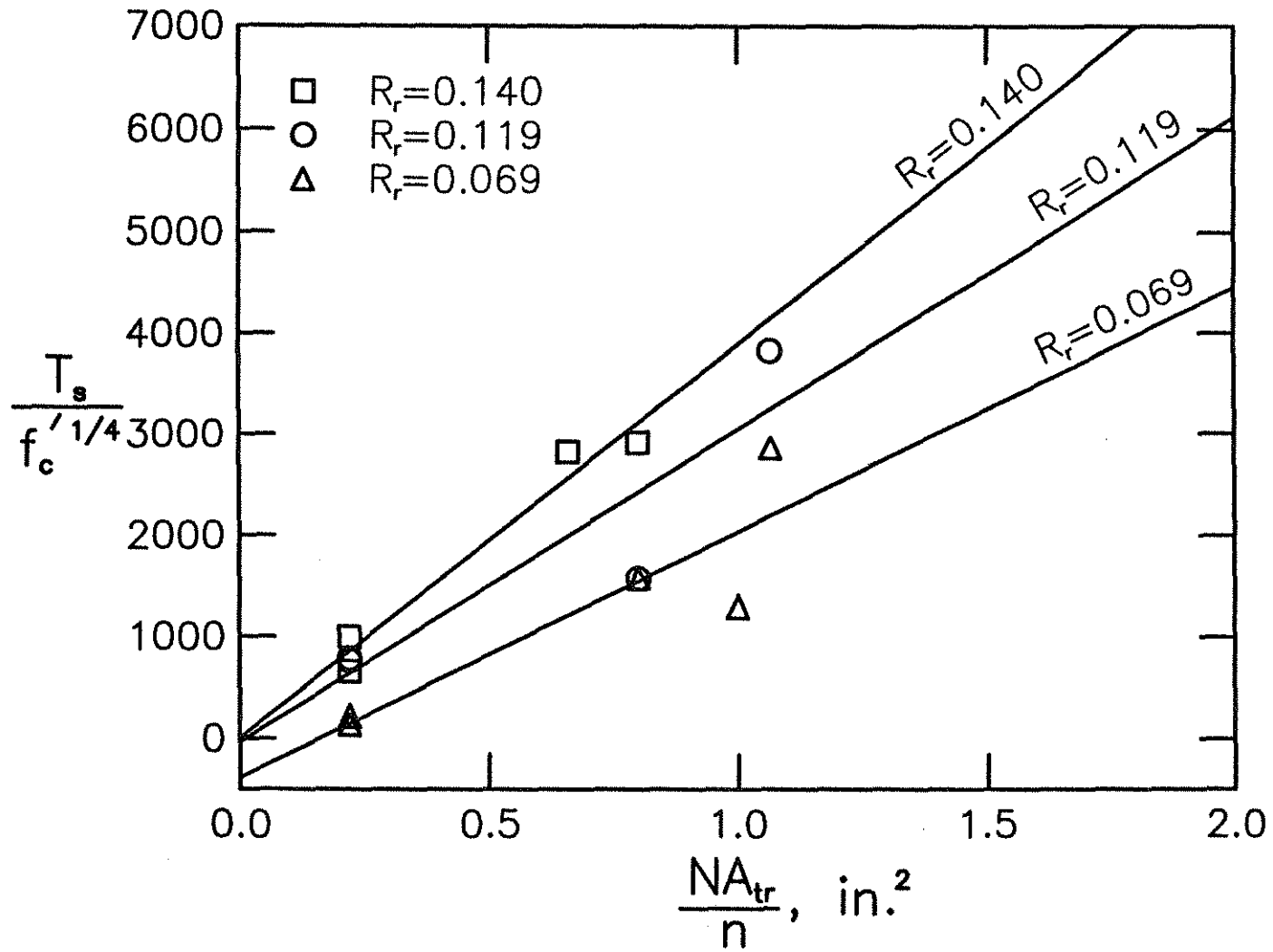


Fig. 6 Increase in bond force,  $T_s$ , normalized with respect to  $f'_c{}^{1/4}$  versus effective transverse reinforcement  $NA_{tr}/n$ , for splices in concrete containing basalt coarse aggregate ( $T_s$  in lb,  $f'_c$  in psi,  $A_{tr}$  in  $\text{in.}^2$ ) (1 lb = 4.45N, 1 psi = 6.89 kPa, 1 in. = 25.4 mm)



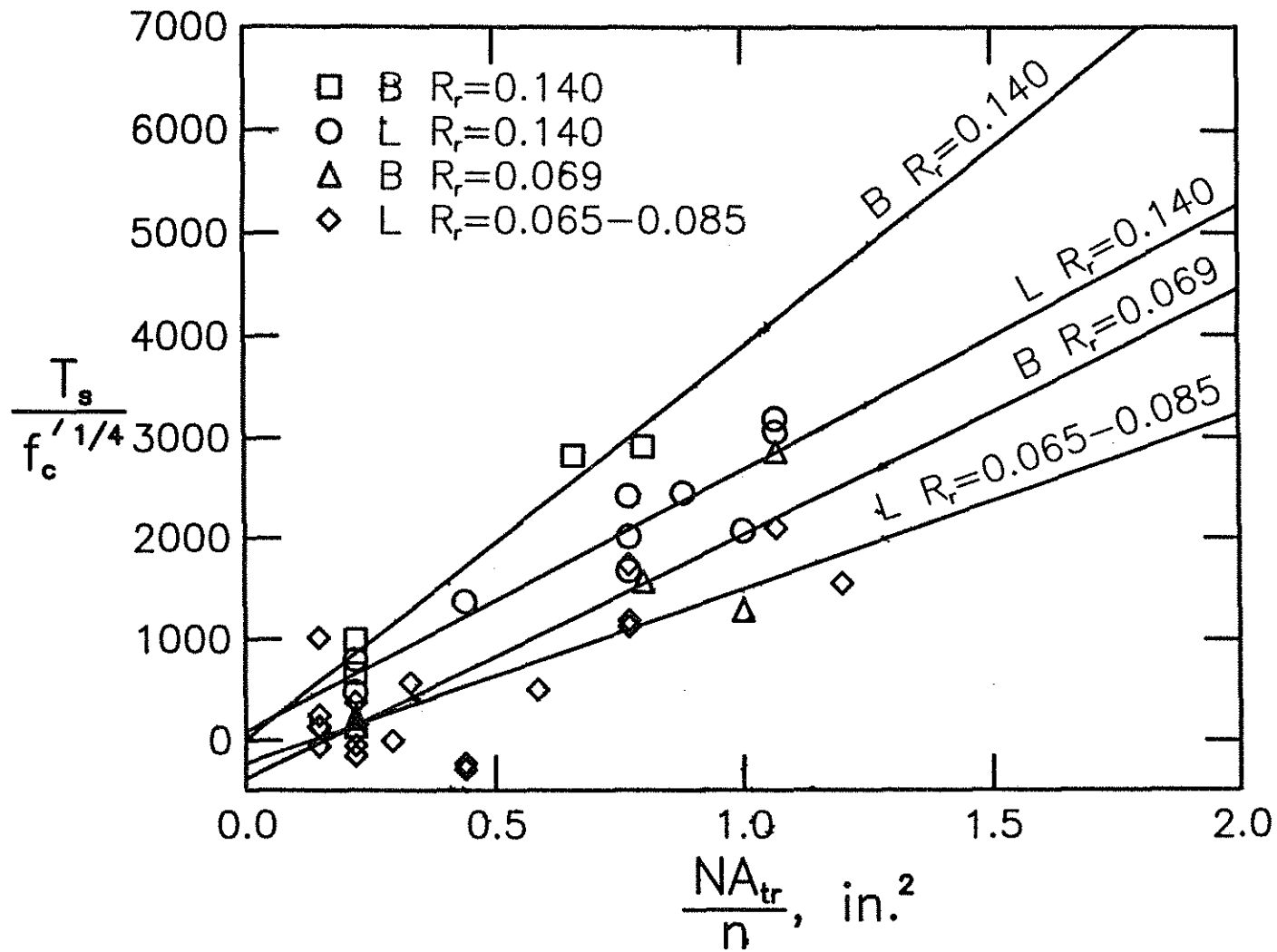


Fig. 7 Comparison of increases in bond force,  $T_s$ , normalized with respect to  $f'_c{}^{1/4}$  for No. 8 (25 mm) bars as affected by coarse aggregate, B = basalt, L = limestone, ( $T_s$  in lb,  $f'_c$  in psi,  $A_{tr}$  in in.<sup>2</sup>) (1 lb = 4.45N, 1 psi = 6.89 kPa, 1 in. = 25.4 mm)

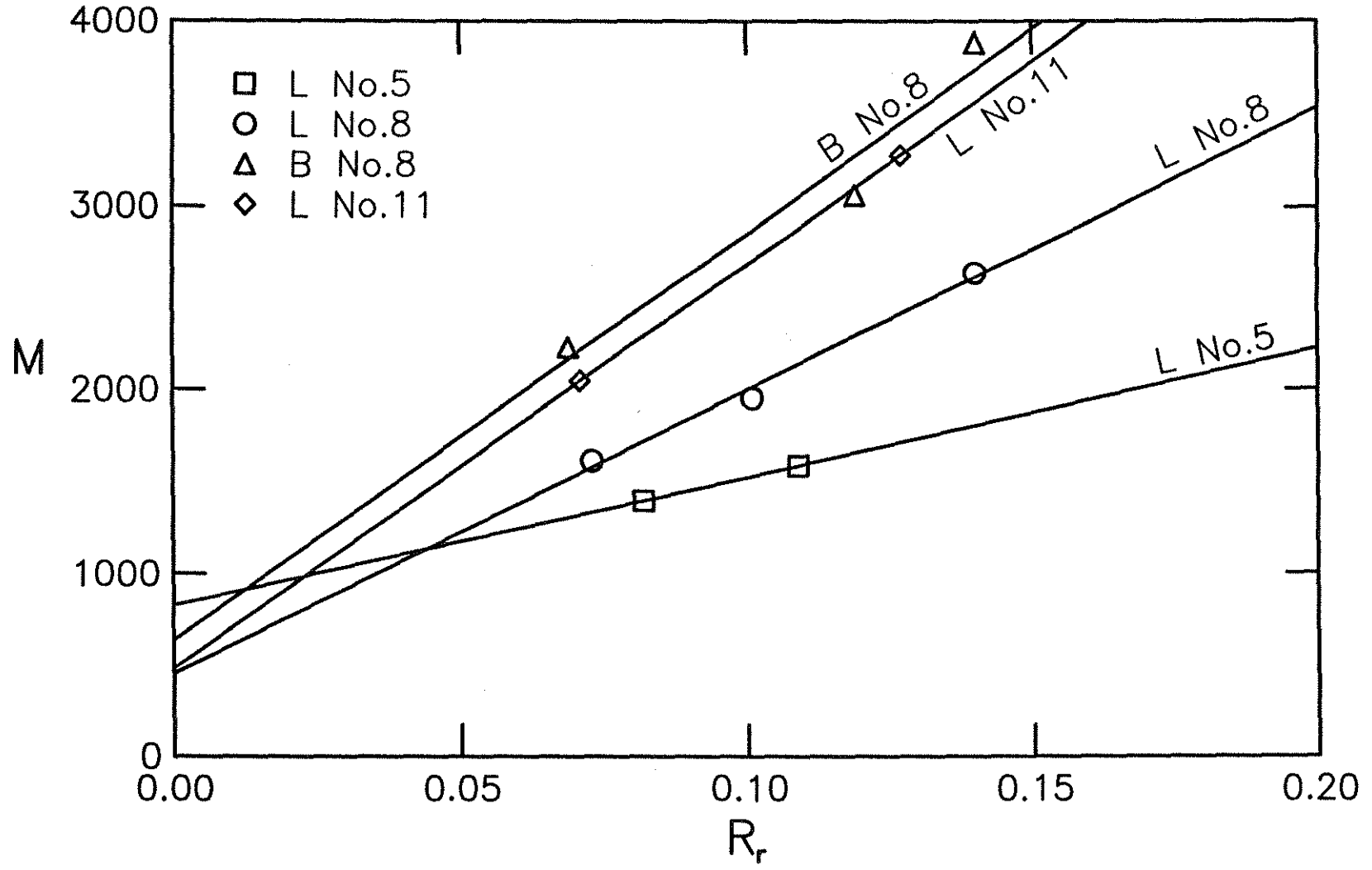


Fig. 8 Mean slope from Eq. 2,  $M$ , versus relative rib area,  $R_r$ , for No. 5, No. 8 and No. 11 (16, 25, and 36 mm) bars cast in concrete containing limestone coarse aggregate (L) and No. 8 (25 mm) bars cast in concrete containing basalt coarse aggregate (B)

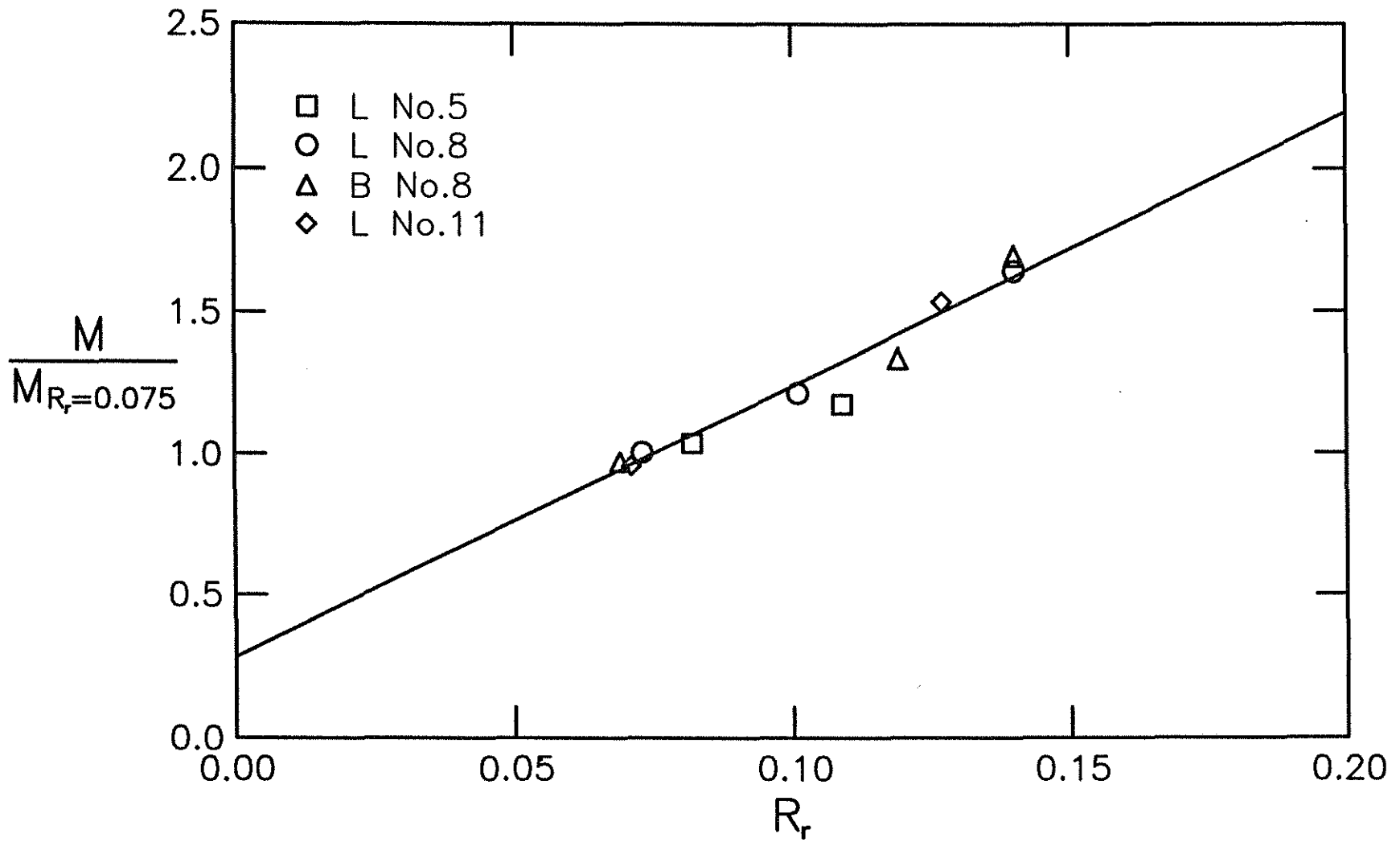


Fig. 9 Factor representing effect of relative rib area on increase in bond strength due to confining reinforcement,  $M/M_{R_r = 0.075}$ , versus relative rib area,  $R_r$

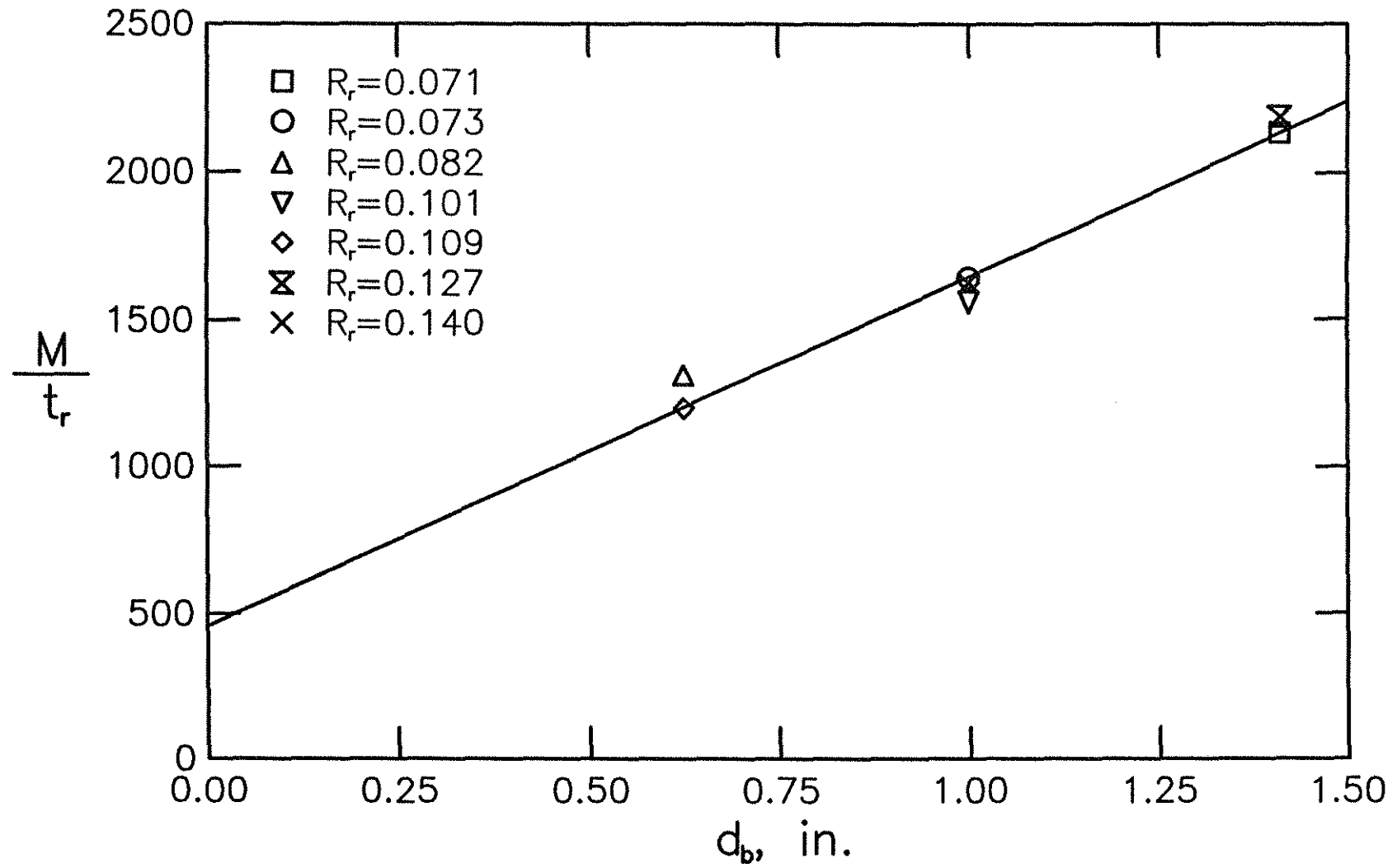


Fig. 10 Mean slope from Eq. 2,  $M$ , normalized with respect to  $t_r = 9.6 R_r + 0.28$  versus nominal bar diameter,  $d_b$  (1 in. = 25.4 mm)

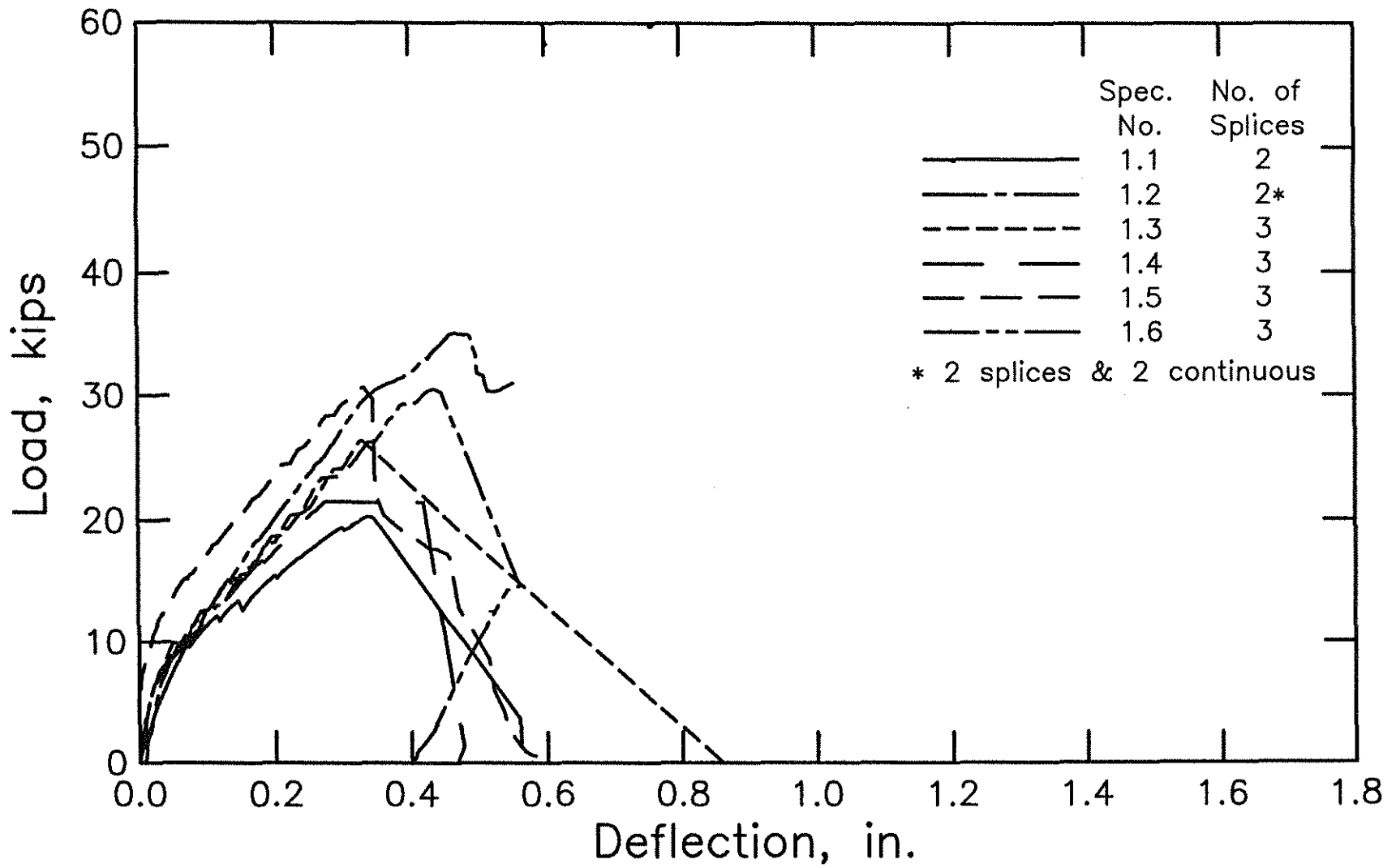


Fig. A.1 Load-deflection curves for splice specimens in Group 1 (1 kip = 4.45 kN, 1 in. = 25.4 mm)

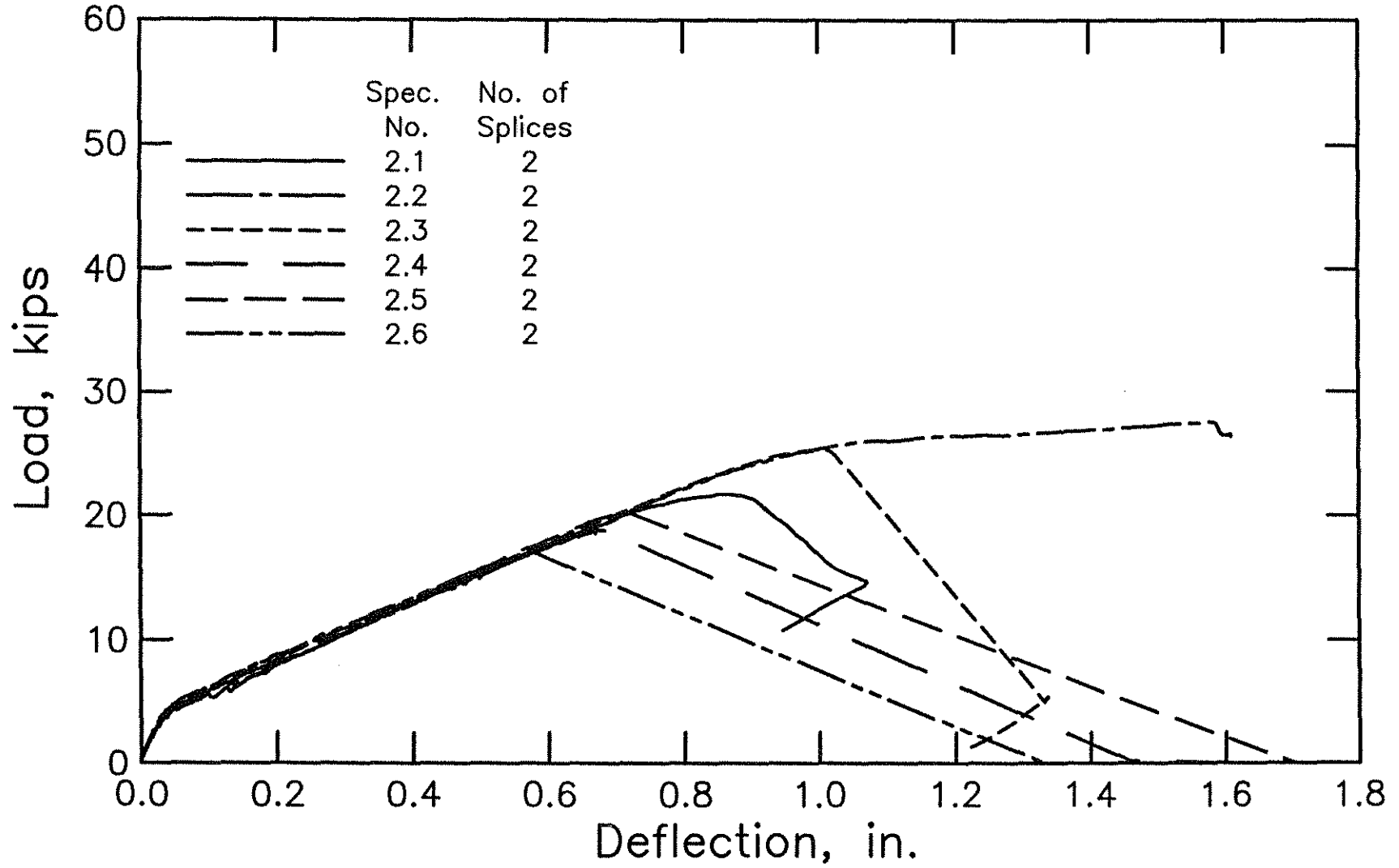


Fig. A.2 Load-deflection curves for splice specimens in Group 2 (1 kip = 4.45 kN, 1 in. = 25.4 mm)

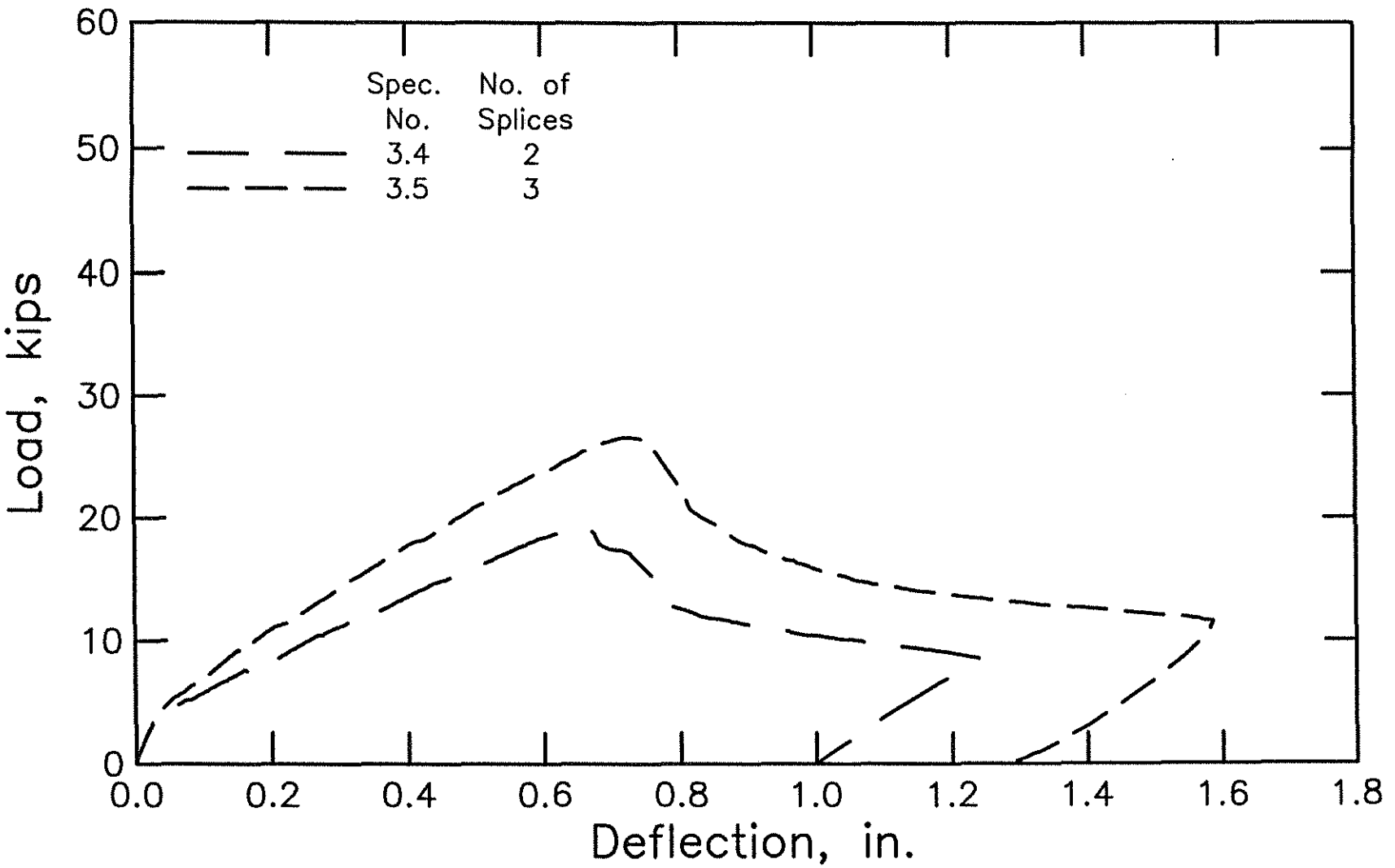


Fig. A.3 Load-deflection curves for splice specimens in Group 3 (1 kip = 4.45 kN, 1 in. = 25.4 mm)

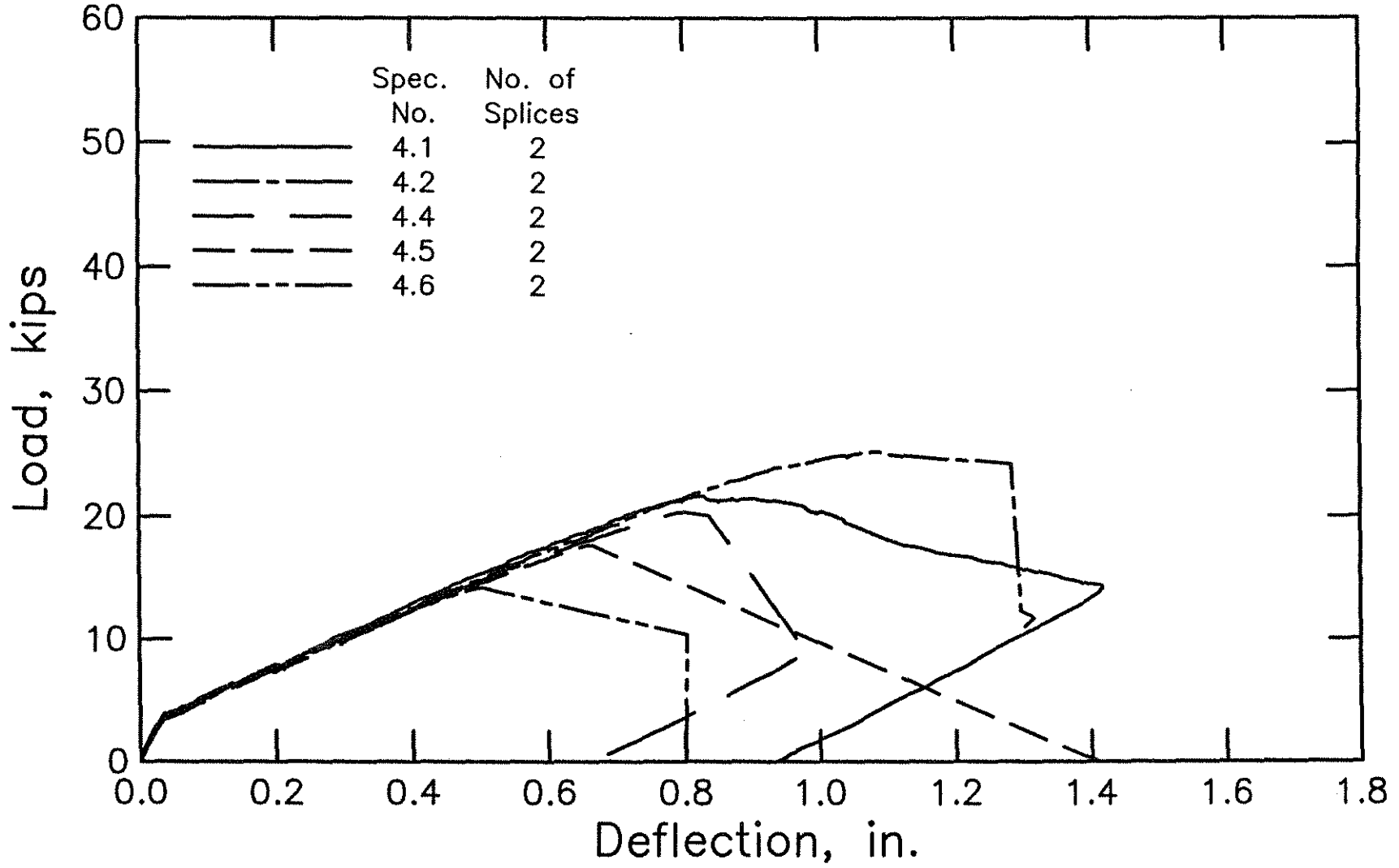


Fig. A.4 Load-deflection curves for splice specimens in Group 4 (1 kip = 4.45 kN, 1 in. = 25.4 mm)



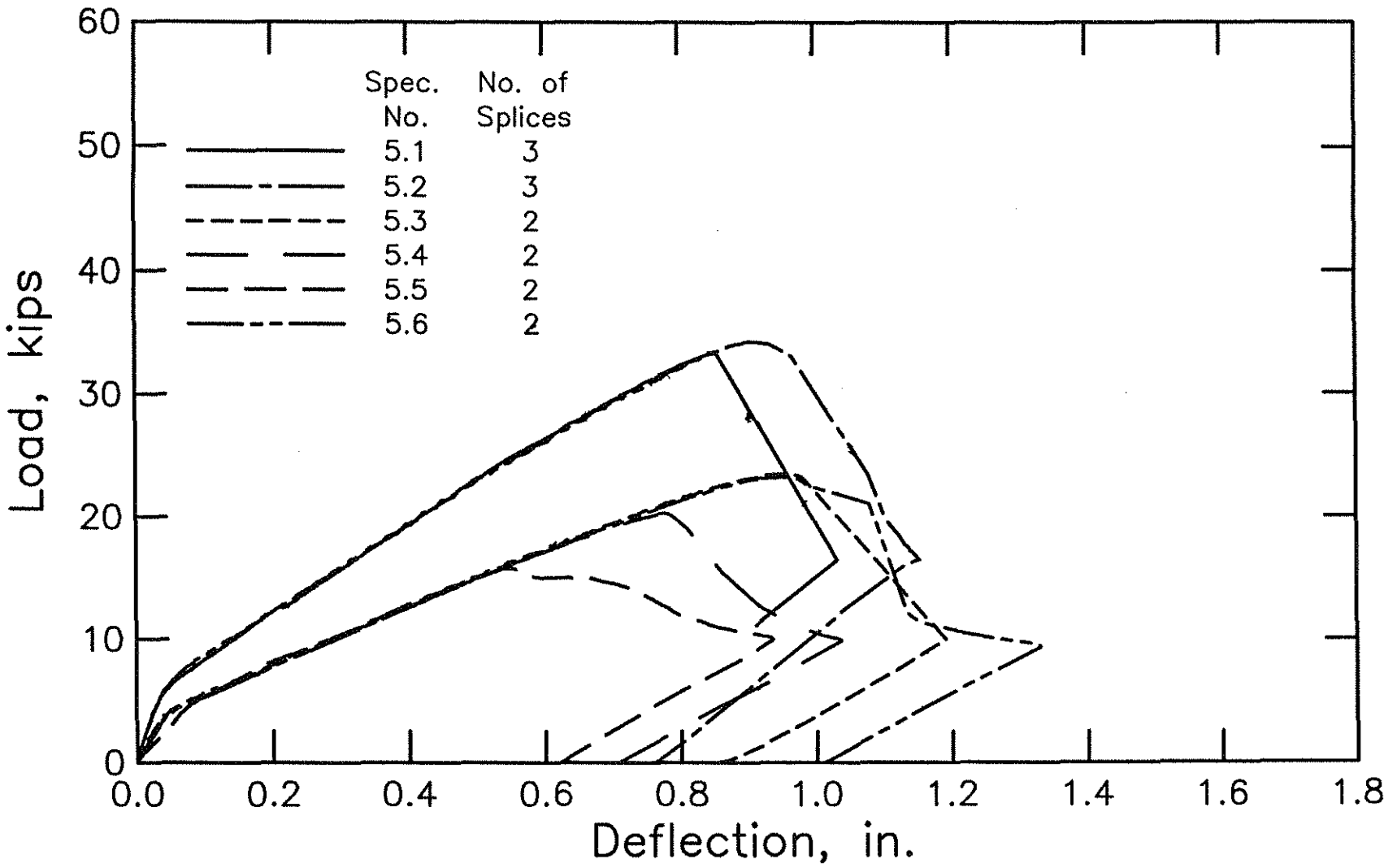


Fig. A.5 Load-deflection curves for splice specimens in Group 5 (1 kip = 4.45 kN, 1 in. = 25.4 mm)

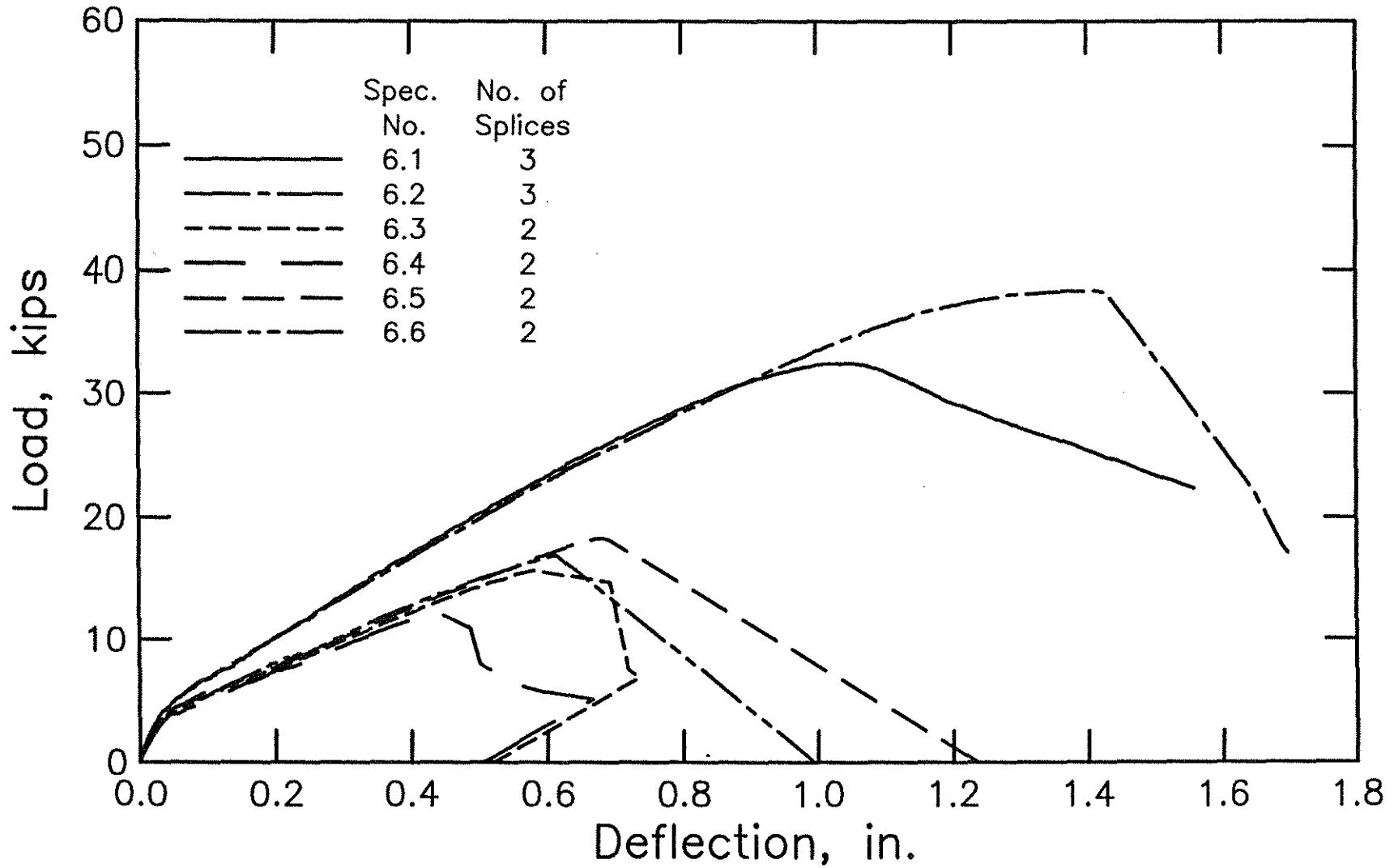


Fig. A.6 Load-deflection curves for splice specimens in Group 6 (1 kip = 4.45 kN, 1 in. = 25.4 mm)

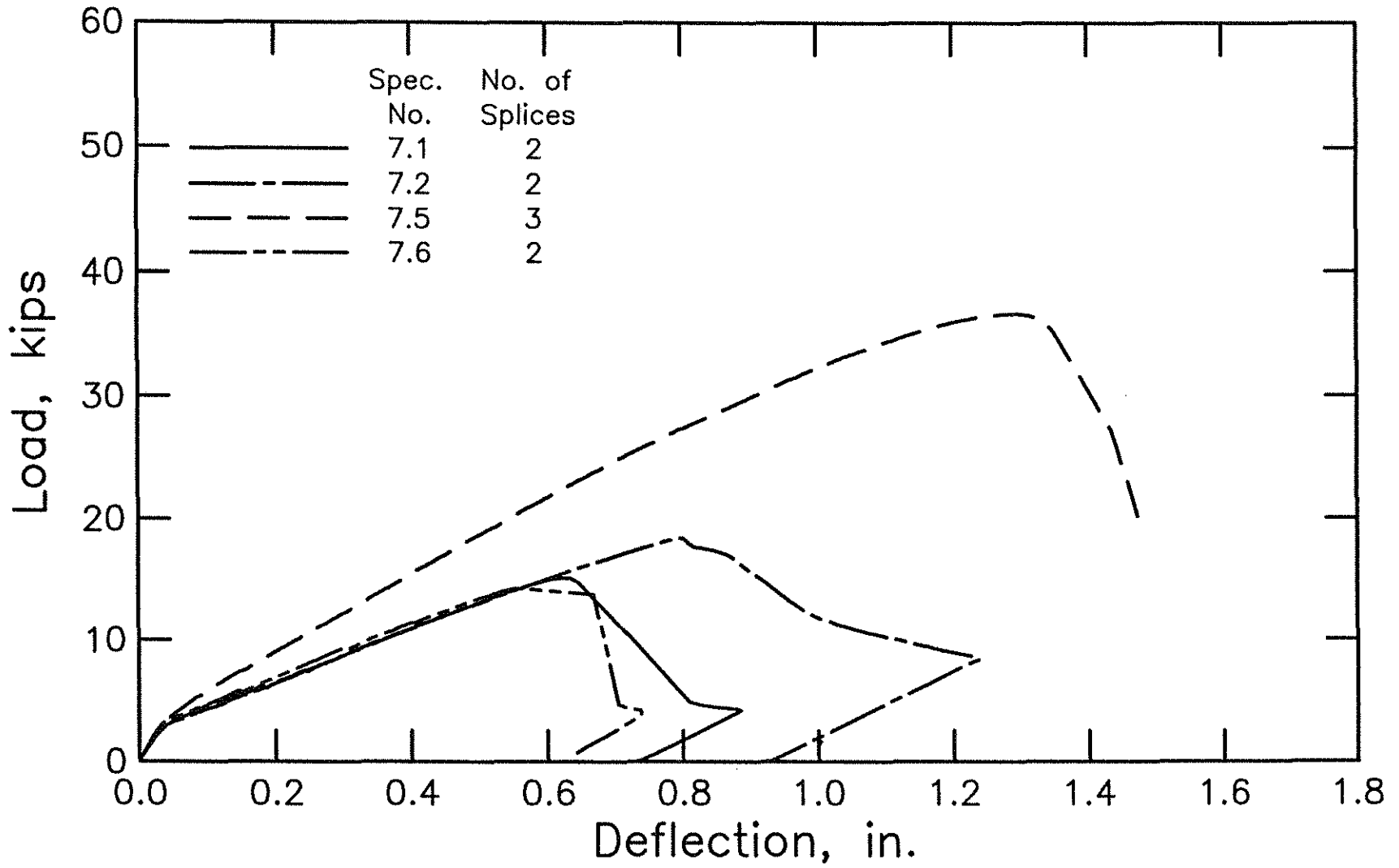


Fig. A.7 Load-deflection curves for splice specimens in Group 7 (1 kip = 4.45 kN, 1 in. = 25.4 mm)

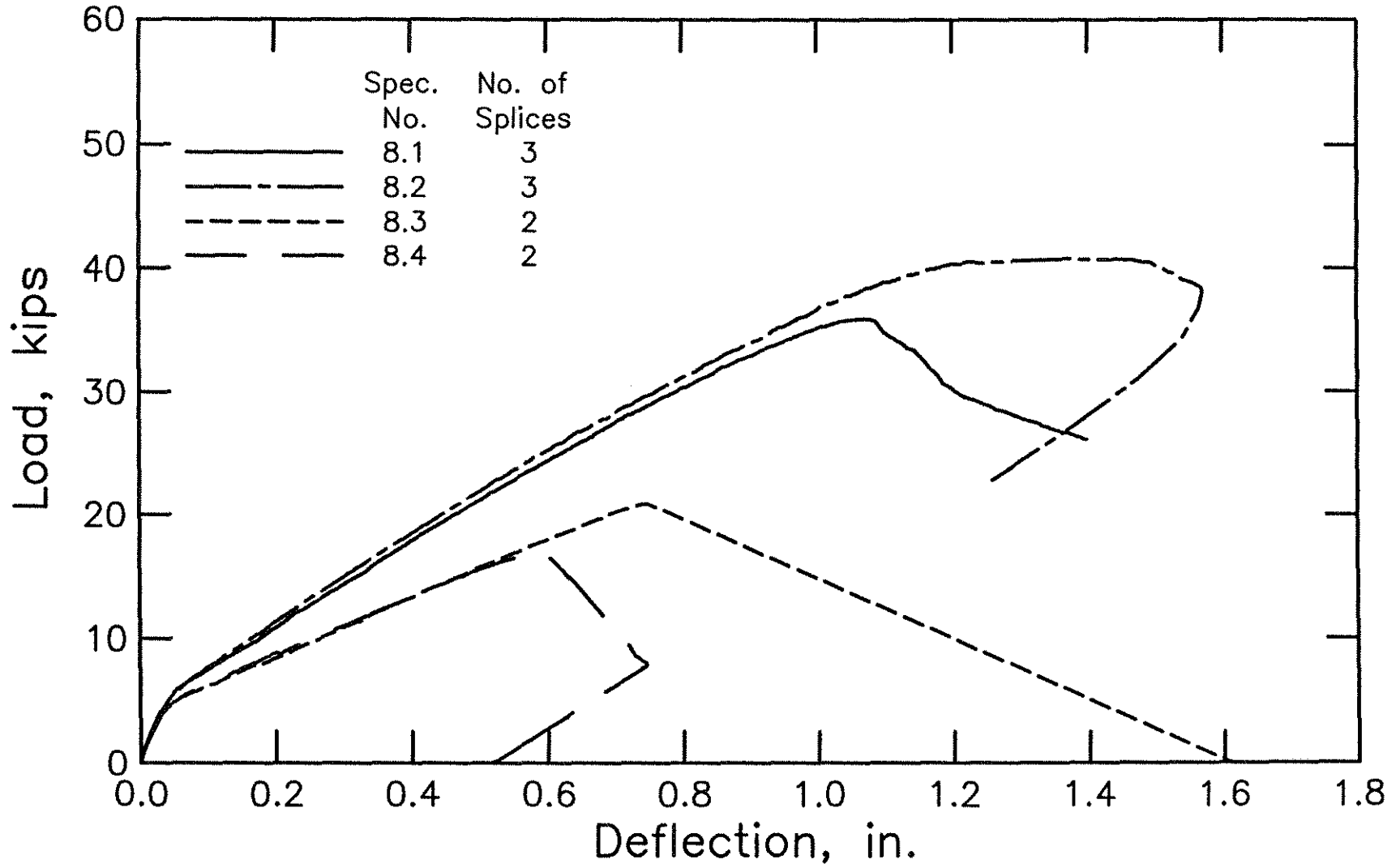


Fig. A.8 Load-deflection curves for splice specimens in Group 8 (1 kip = 4.45 kN, 1 in. = 25.4 mm)

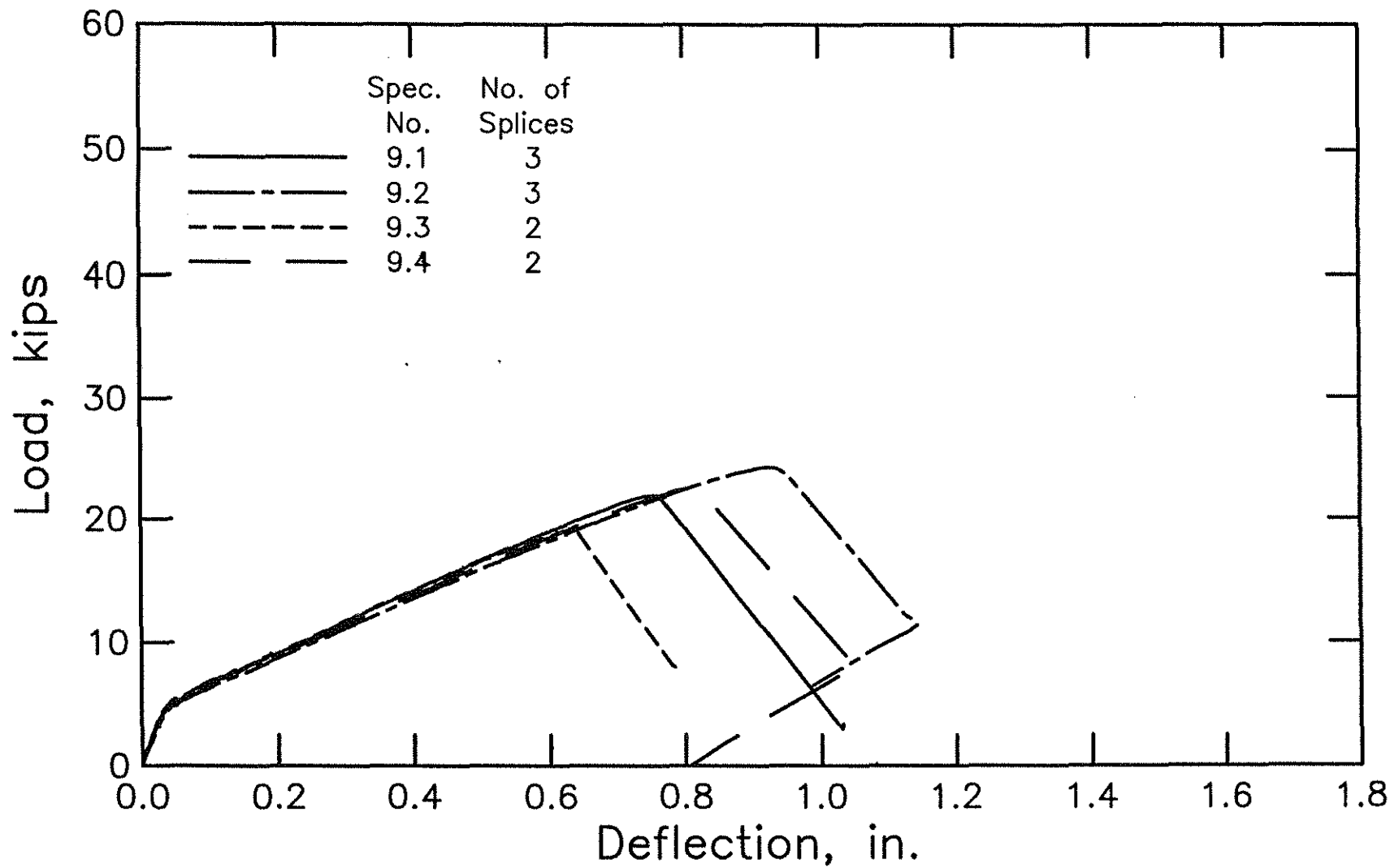


Fig. A.9 Load-deflection curves for splice specimens in Group 9 (1 kip = 4.45 kN, 1 in. = 25.4 mm)

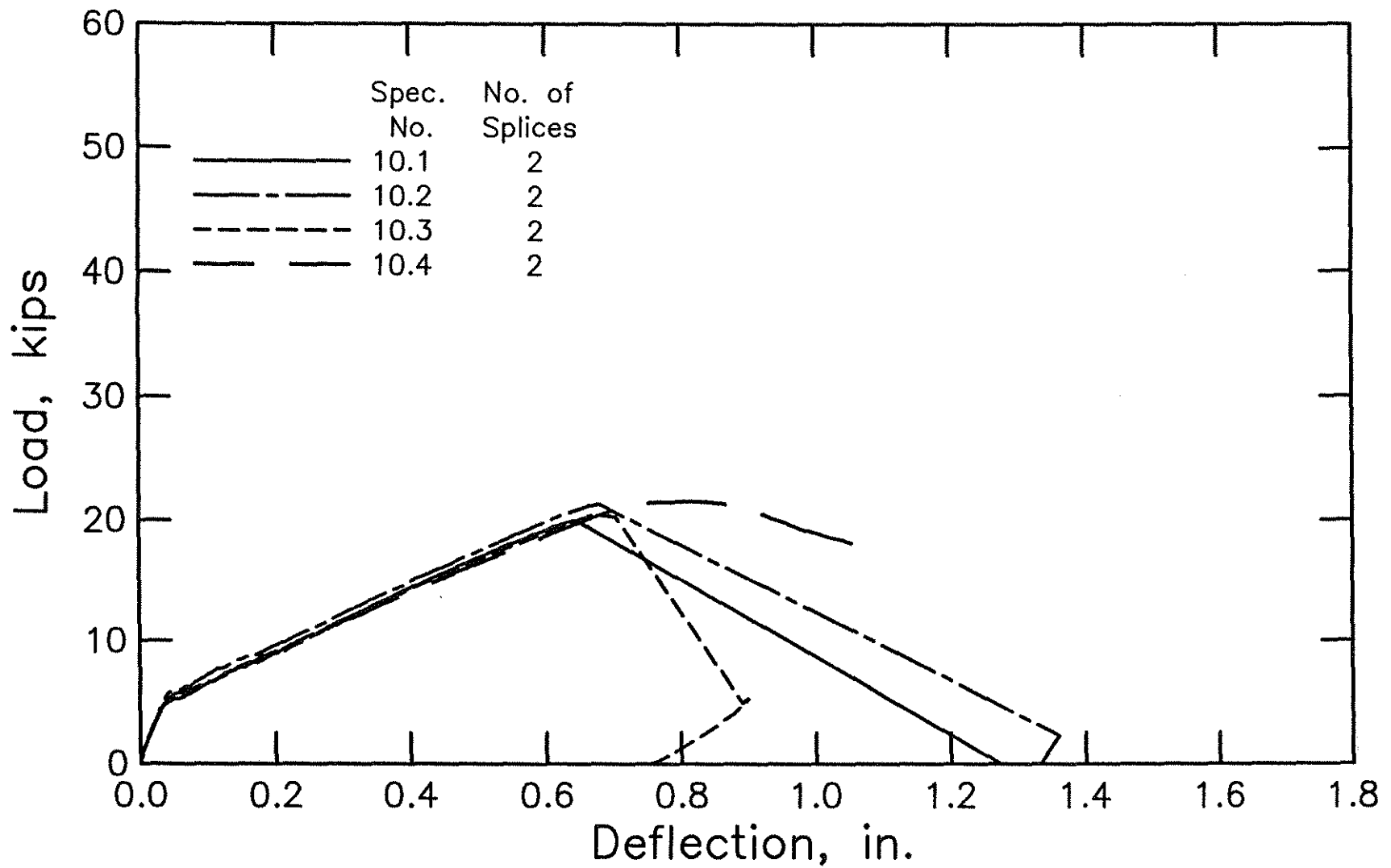


Fig. A.10 Load-deflection curves for splice specimens in Group 10 (1 kip = 4.45 kN, 1 in. = 25.4 mm)

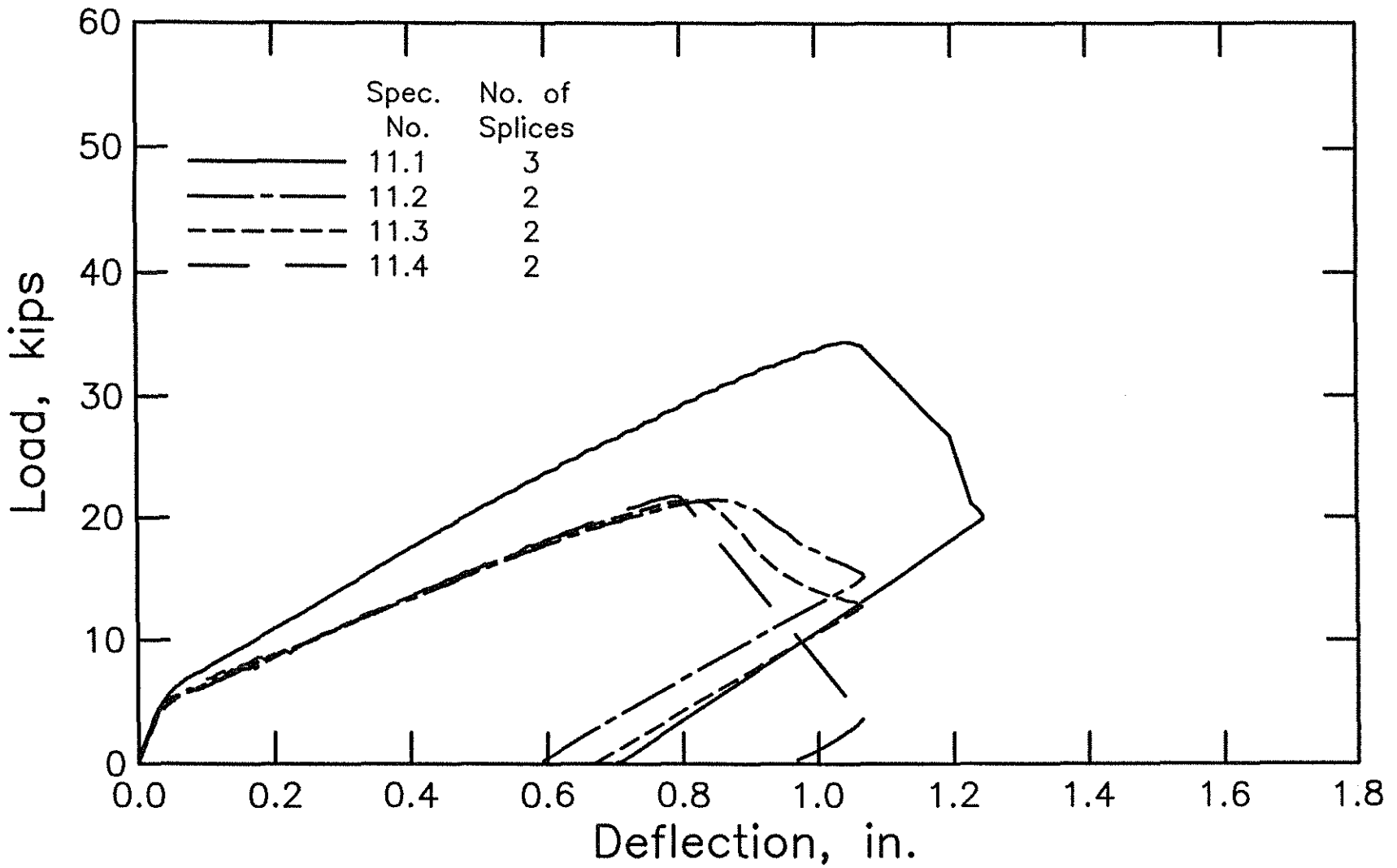


Fig. A.11 Load-deflection curves for splice specimens in Group 11 (1 kip = 4.45 kN, 1 in. = 25.4 mm)

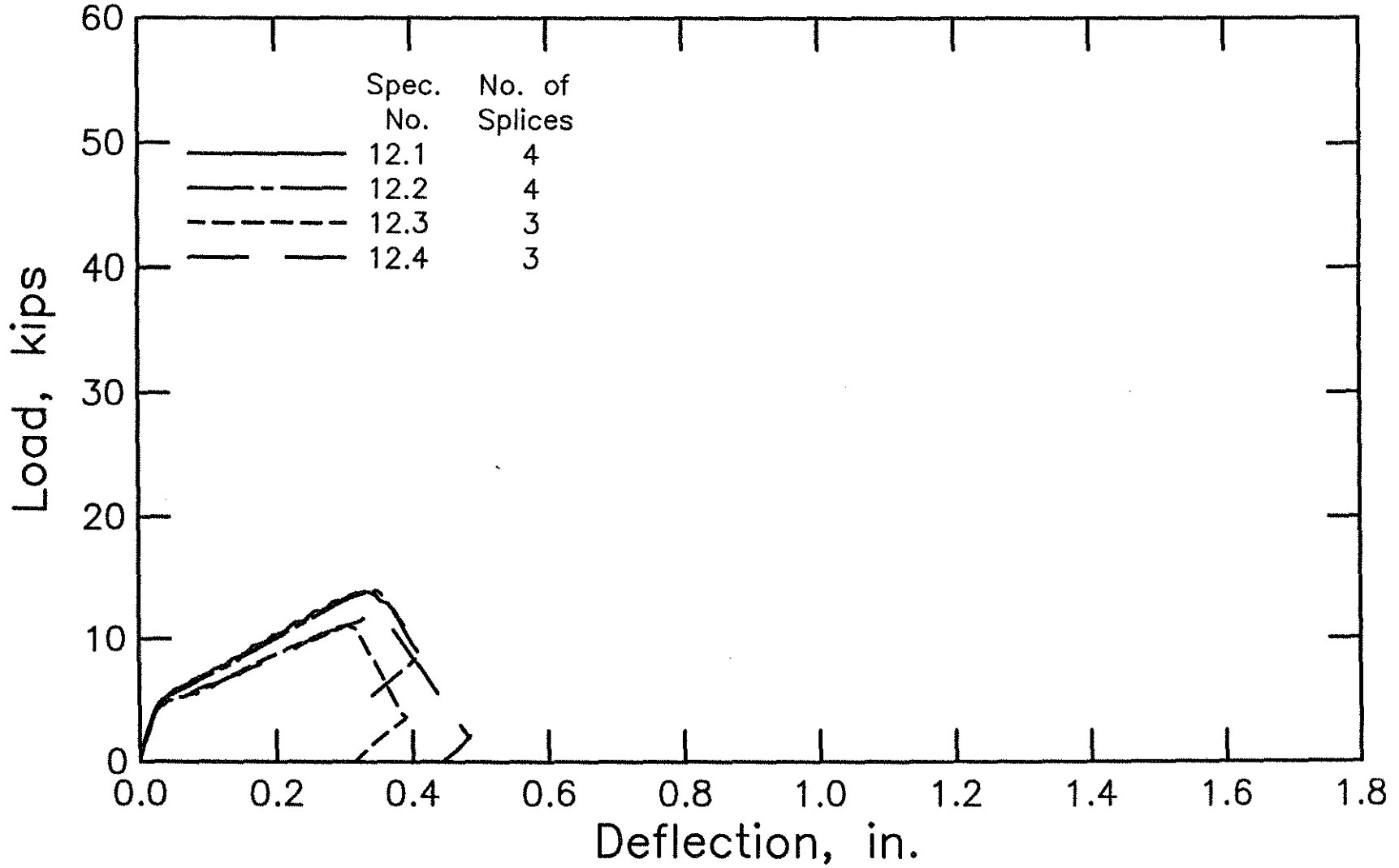


Fig. A.12 Load-deflection curves for splice specimens in Group 12 (1 kip = 4.45 kN, 1 in. = 25.4 mm)



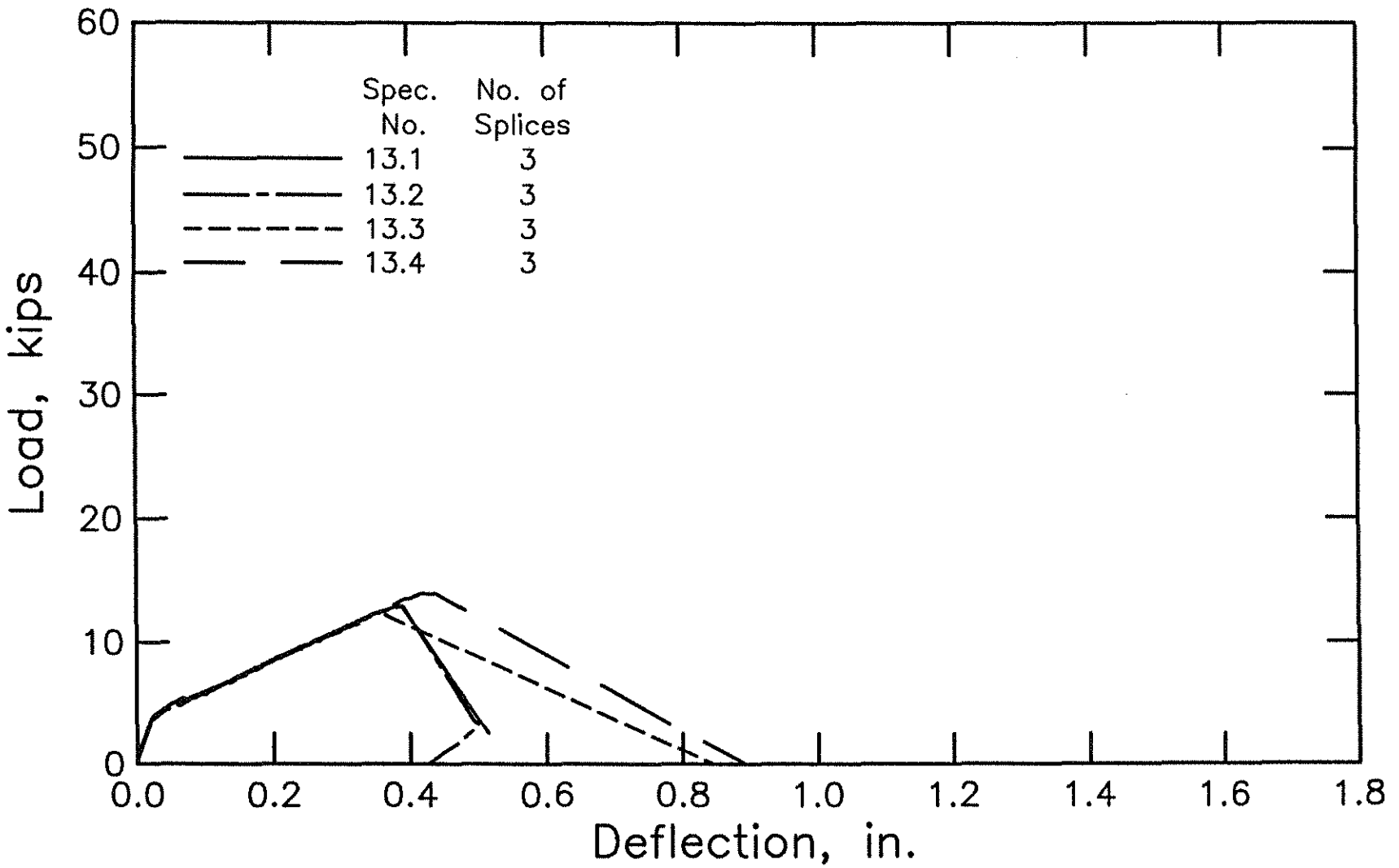


Fig. A.13 Load-deflection curves for splice specimens in Group 13 (1 kip = 4.45 kN, 1 in. = 25.4 mm)

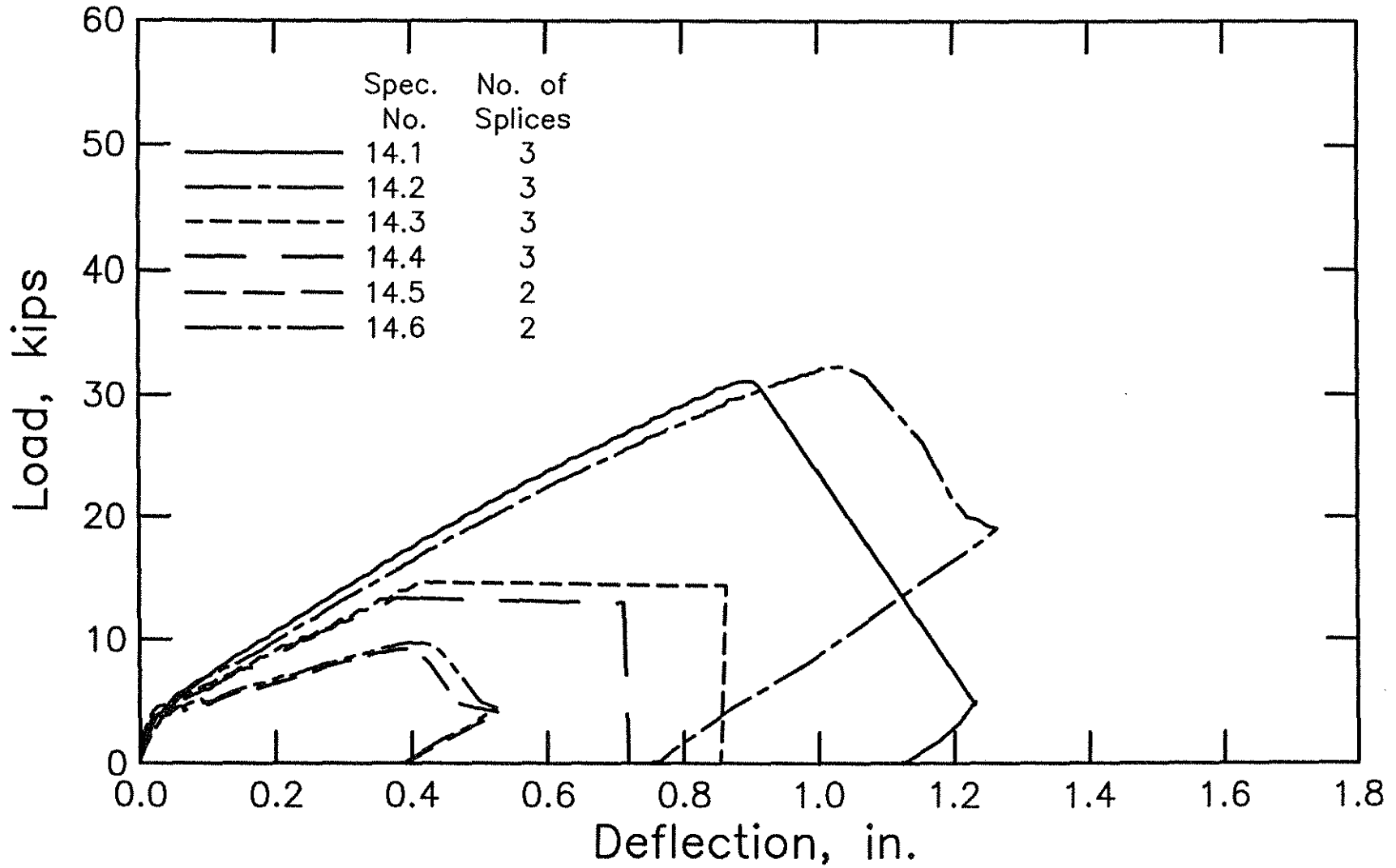


Fig. A.14 Load-deflection curves for splice specimens in Group 14 (1 kip = 4.45 kN, 1 in. = 25.4 mm)

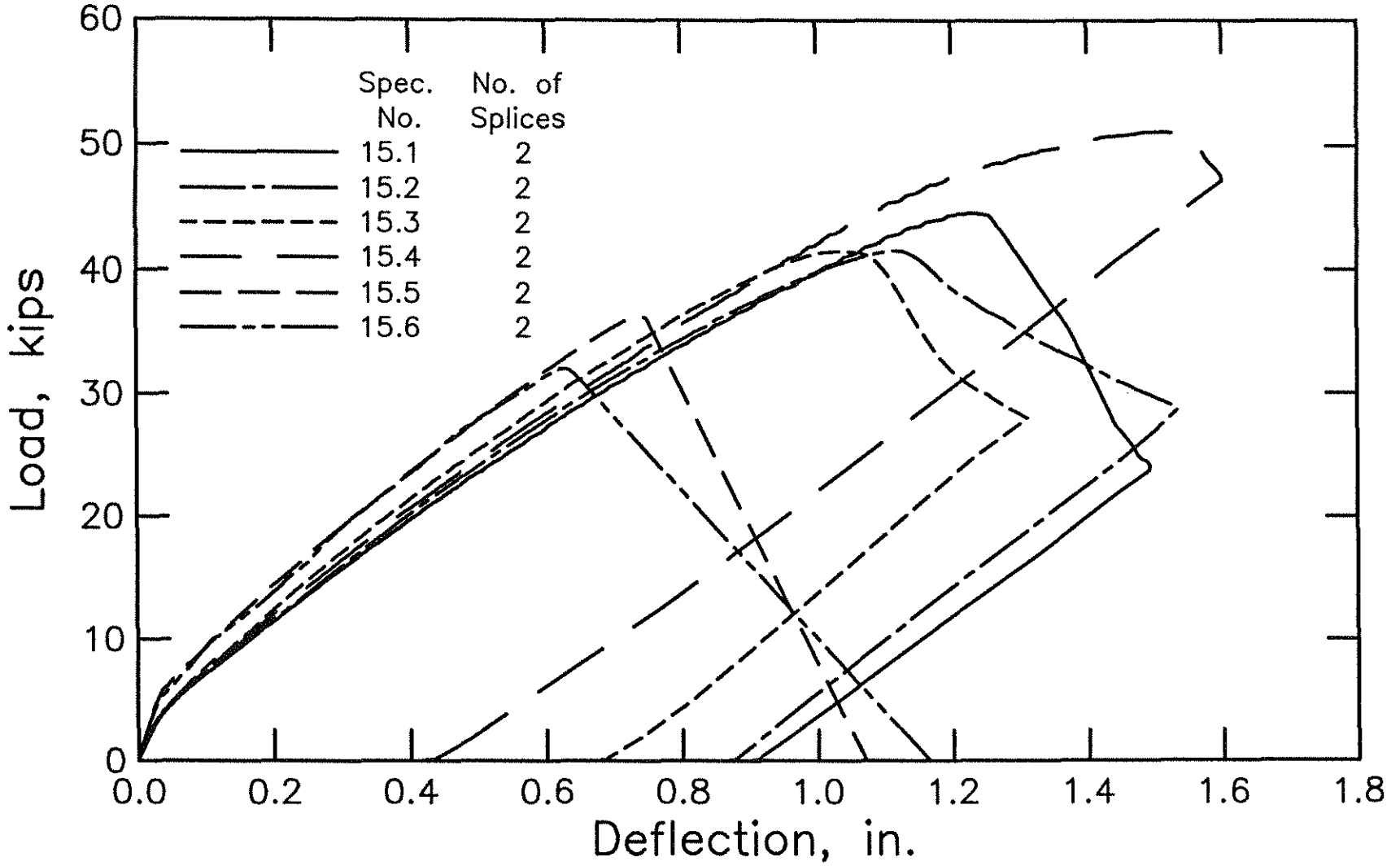


Fig. A.15 Load-deflection curves for splice specimens in Group 15 (1 kip = 4.45 kN, 1 in. = 25.4 mm)

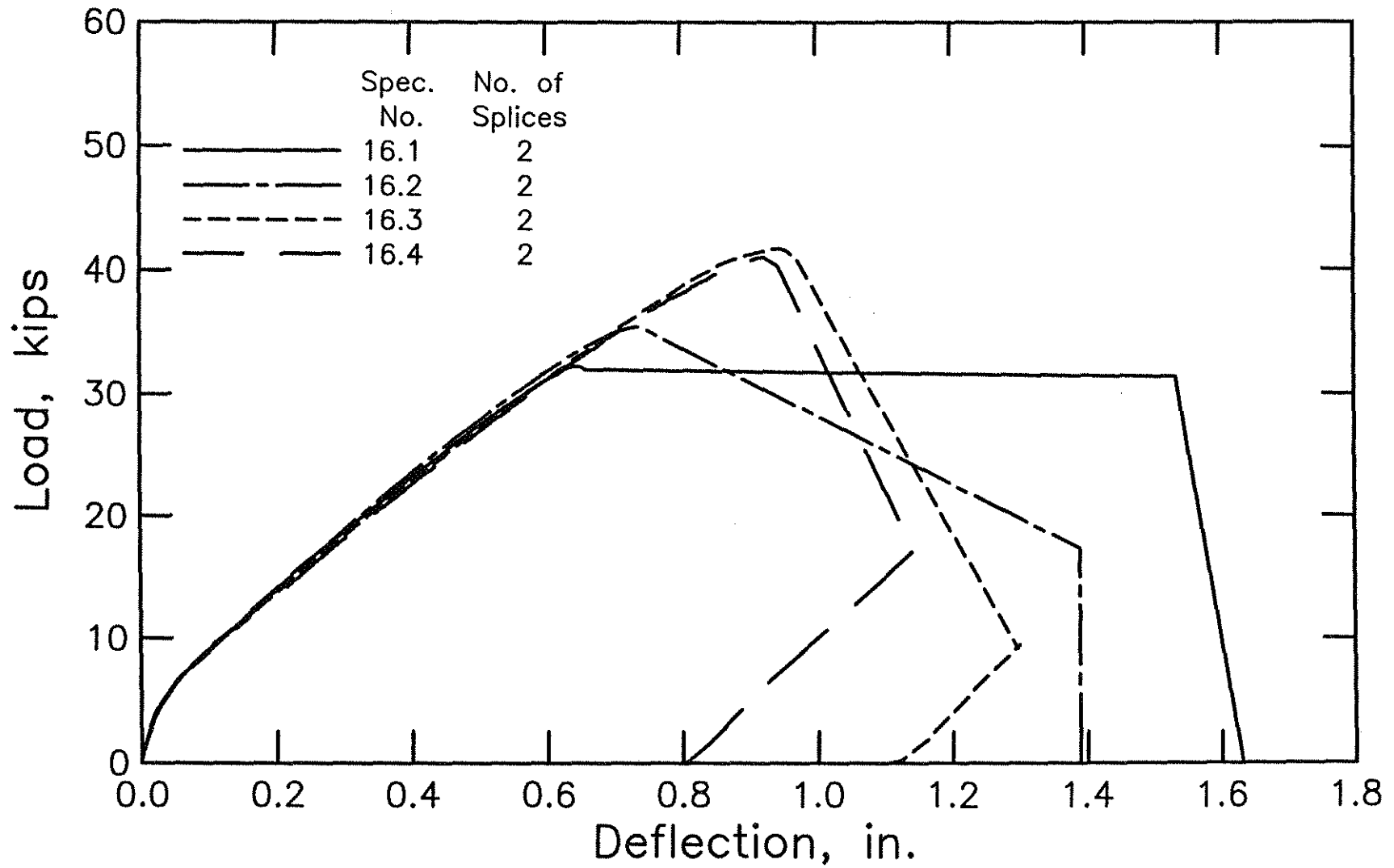


Fig. A.16 Load-deflection curves for splice specimens in Group 16 (1 kip = 4.45 kN, 1 in. = 25.4 mm)

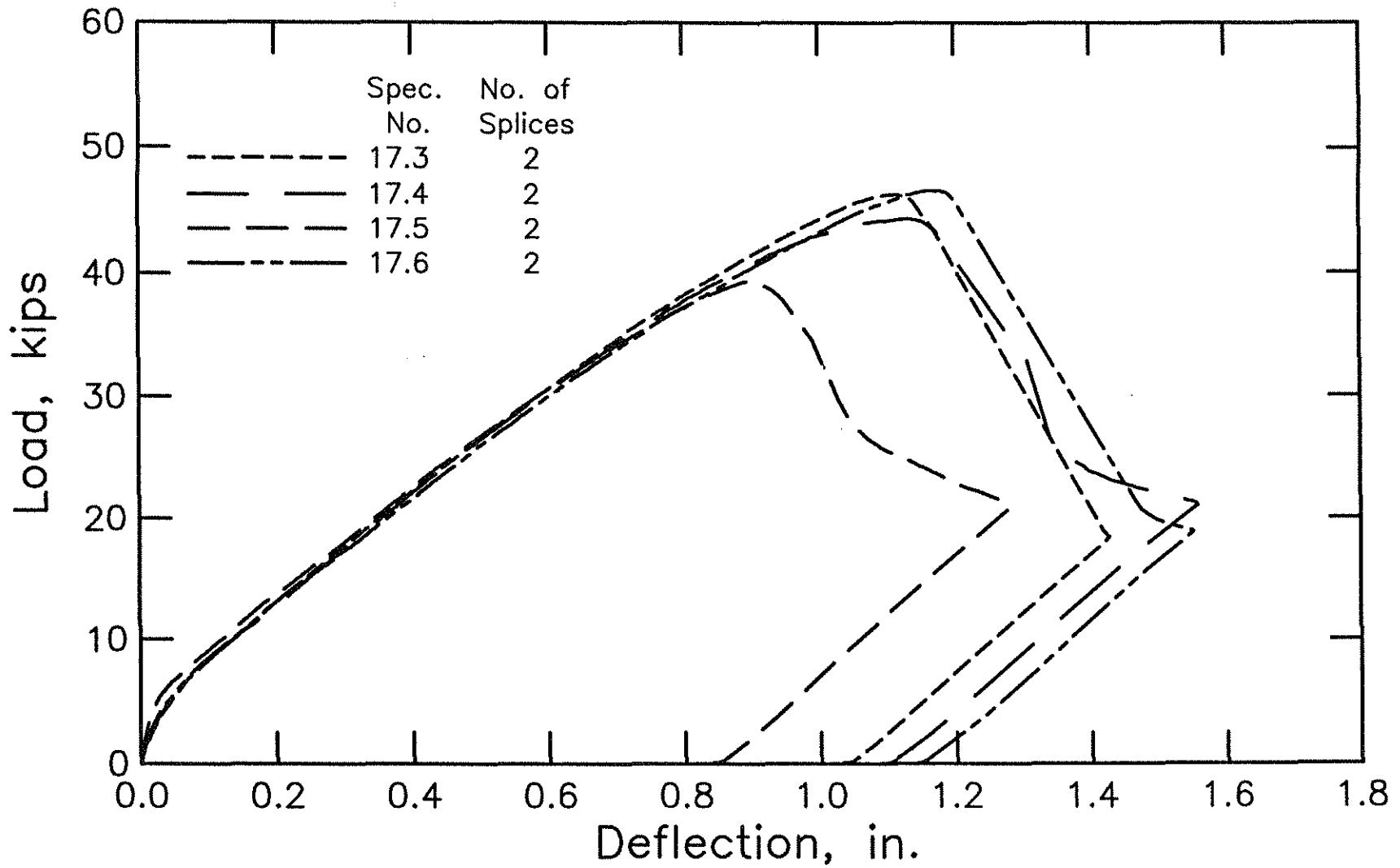


Fig. A.17 Load-deflection curves for splice specimens in Group 17 (1 kip = 4.45 kN, 1 in. = 25.4 mm)

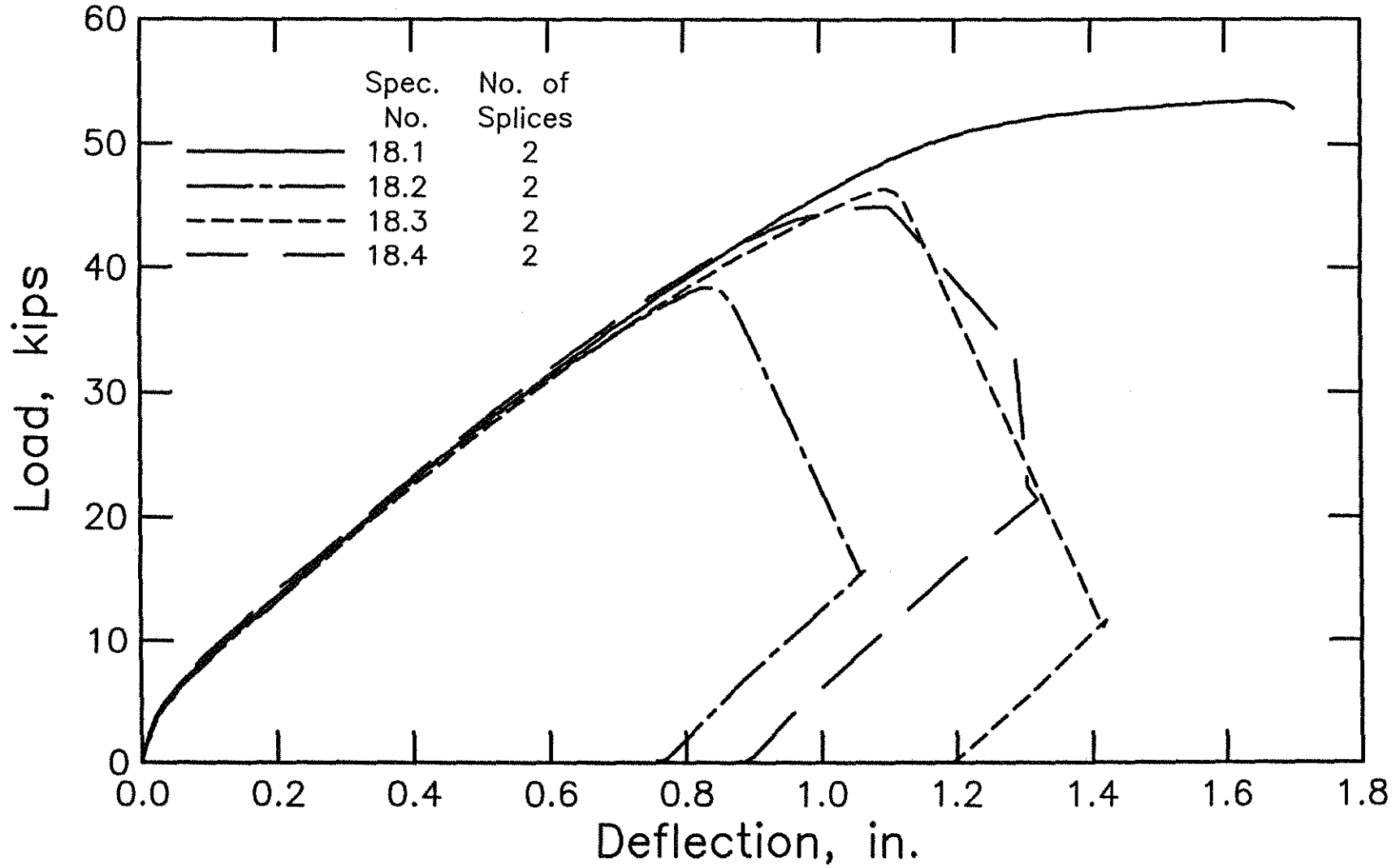


Fig. A.18 Load-deflection curves for splice specimens in Group 18 (1 kip = 4.45 kN, 1 in. = 25.4 mm)

## Appendix B

### Table B.1

**Splice specimen properties and test results from Hester et al. 1991**

Specimen No. +	Bar ++	Relative Rib Area	n	$l_s$ (in.)	$d_b$ (in.)	$c_{so}$ (in.)	$c_{sl}$ (in.)	$c_b$ (in.)	b (in.)	h (in.)	l (ft)	$l_c$ (ft)	d (in.)	$f'_c$ (psi)	N	$d_s$ (in.)	$f_{yt}$ (ksi)	$M_u$ (k-in.)	$f_s$ +++ (ksi)
1.2	8N0	0.078	3	16.00	1.000	2.000	1.500	2.000	16.00	16.00	13.00	4.00	13.50	5990	2	0.375	77.30	1604	56.00
2.2	8C0	0.071	3	16.00	1.000	2.000	1.500	1.830	16.00	16.28	13.00	4.00	13.95	6200	2	0.375	54.10	1305	43.99
3.2	8S0	0.070	3	16.00	1.000	2.000	1.500	2.080	16.06	16.24	13.00	4.00	13.66	6020	2	0.375	68.90	1348	46.47
4.2	8S0	0.070	3	16.00	1.000	2.000	1.500	2.040	16.09	16.36	13.00	4.00	13.82	6450	2	0.375	68.90	1384	47.06
4.3	8S0	0.070	3	16.00	1.000	2.000	1.500	2.100	16.09	16.28	13.00	4.00	13.68	6450	3	0.375	68.90	1456	50.04
5.2	8C0	0.071	3	16.00	1.000	2.000	1.500	2.060	16.10	16.42	13.00	4.00	13.86	5490	2	0.375	54.10	1367	46.51
5.3	8C0	0.071	3	16.00	1.000	2.000	1.500	2.060	16.09	16.12	13.00	4.00	13.56	5490	3	0.375	54.10	1244	43.31
6.2	8C0	0.071	3	22.75	1.000	2.000	1.500	2.170	16.06	16.20	13.00	4.00	13.53	5850	3	0.375	54.10	1620	56.45
6.3	8C0	0.071	3	22.75	1.000	2.000	1.500	2.160	16.03	16.17	13.00	4.00	13.51	5850	4	0.375	54.10	1595	55.67
7.2	8C0	0.071	2	16.00	1.000	2.000	4.000	2.030	16.00	16.30	13.00	4.00	13.77	5240	3	0.375	54.10	1019	51.49

+ Specimen No.  
G.P, G = group number (1-7), P = casting order in the group (1-3)

++ Bar Designation  
#AA, # = bar size (No. 5, No. 8 or No. 11), AA = bar manufacturer and deformation pattern

C0 Conventional Chaparral Steel bar  
N0 Conventional North Star Steel bar  
S0 Conventional Structural Metals, Inc. bar

+++ Bar stress is computed based on working stress if  $f_s$  does not exceed bar yield stress, otherwise computed based on ultimate strength.  
 $M_u$  and  $f_s$  include effect of beam self weight and loading system.

1 in. = 25.4 mm; 1 ft = 305 mm; 1 psi = 6.89 kPa; 1 ksi = 6.89 MPa; 1 kip = 4.45 kN; 1 k-in. = 0.113 kN-m

## Appendix C

## Notation

$A_b$	= bar area, in in. <sup>2</sup>
$A_{tr}$	= area of each stirrup or tie crossing the potential plane of splitting adjacent to the reinforcement being developed or spliced, in in. <sup>2</sup>
$b$	= intercepts of the best-fit lines relating $T_v/f'_c{}^{1/4}$ to $NA_{tr}/n$ in Figs. 5 and 6 or beam width in Table 1, in in.
$c$	= $c_m + 0.5 d_b$
$c_b$	= bottom cover of reinforcing bars, in in.
$c_M$	= maximum value of $c_s$ or $c_b$ ( $c_M/c_m \leq 3.5$ ), in in.
$c_m$	= minimum value of $c_s$ or $c_b$ ( $c_M/c_m \leq 3.5$ ), in in.
$c_s$	= $\min(c_{si} + 0.25 \text{ in.}, c_{so})$ or $\min(c_{si}, c_{so})$ , in in.
$c_{si}$	= one-half of clear spacing between bars, in in.
$c_{so}$	= side cover of reinforcing bars, in in.
$d$	= beam effective depth, in in.
$d_b$	= nominal bar diameter, in in.
$d_s$	= stirrup diameter, in in.
$f'_c$	= concrete compressive strength, in psi; $f'_c{}^{1/4}$ in psi
$f_s$	= steel stress at failure, in psi
$f_y$	= yield strength of bars being spliced or developed, in psi
$f_{yt}$	= yield strength of transverse reinforcement, in ksi
$h$	= beam depth, in in.
$K_{tr}$	= $K_{tr}(\text{conv.}) = 34.5 (0.72 d_b + 0.28)A_{tr}/sn$ for conventional reinforcement (average $R_r = 0.0727$ ) = $K_{tr}(\text{new}) = 53 (0.72 d_b + 0.28)A_{tr}/sn$ for new reinforcement (average $R_r = 0.1275$ )
$l$	= beam length, in ft
$l_c$	= length of constant moment region, in ft
$l_d$	= development or splice length, in in.



- $l_s$  = splice length, in in.  
 $M$  = slope of the modified relationship in Eq. 2  
 $M_{R_r = 0.075}$  = value of  $M$  at  $R_r=0.075$   
 $M_u$  = moment at splice failure, in kip-in.  
 $m$  = slopes of the best-fit lines relating  $T_s/f'_c{}^{1/4}$  to  $NA_{tr}/n$  in Figs. 5 and 6  
 $N$  = number of transverse reinforcing bars (stirrups or ties) crossing  $l_d$   
 $n$  = number of bars being developed or spliced along the plane of splitting  
 $P$  = total applied load at splice failure, in kips  
 $R_r$  = ratio of projected rib area normal to bar axis to the product of the nominal bar perimeter and the center-to-center rib spacing  
 $s$  = spacing of transverse reinforcement, in in.  
 $T_b$  = total force in a bar at splice failure, in lb  
 $T_c$  = concrete contribution to total force in a bar at splice failure, in lb  
 $T_s$  = confining steel contribution to total force in a bar at splice failure, in lb  
 $t_d$  = term representing the effect of bar size on  $T_s$   
 $t_r$  = term representing the effect of relative rib area on  $T_s$